Stem Cell Reports
Article

OPEN ACCESS

Generation of TCR-Expressing Innate Lymphoid-like Helper Cells that Induce Cytotoxic T Cell-Mediated Anti-leukemic Cell Response

Norihiro Ueda,[1,2,4] Yasushi Uemura,[3,4,*] Rong Zhang,[3,4] Shuichi Kitayama,[1] Shoichi Iriguchi,[1] Yohei Kawai,[1] Yutaka Yasui,[1] Minako Tatsumi,[4] Tatsuki Ueda,[1] Tian-Yi Liu,[4,5] Yasutaka Mizoro,[6] Chihiro Okada,[6] Akira Watanabe,[6] Mahito Nakanishi,[7] Satoru Senju,[8] Yasuharu Nishimura,[8] Kiyotaka Kuzushima,[4,9] Hitoshi Kiyoi,[2] Tomoki Naoe,[10] and Shin Kaneko[1,*]

[1]Shin Kaneko Laboratory, Department of Cell Growth and Differentiation, Center for iPS Cell Research and Application (CiRA), Kyoto University, 53 Shogoin Kawahara-cho, Sakyo-ku, Kyoto 606-8501, Japan
[2]Department of Hematology and Oncology, Nagoya University Graduate School of Medicine, 65 Tsurumai-cho, Showa-ku, Nagoya 466-8550, Japan
[3]Division of Cancer Immunotherapy, Exploratory Oncology Research & Clinical Trial Center, National Cancer Center (NCC), 6-5-1 Kashiwanoha, Kashiwa, Chiba 277-8577, Japan
[4]Division of Immunology, Aichi Cancer Center Research Institute (ACCRI), 1-1 Kanokoden, Chikusa-ku, Nagoya 464-8681, Japan
[5]Key Laboratory of Cancer Center, Chinese PLA General Hospital, 28 Fuxing Road, Beijing 100853, China
[6]Department of Life Science Frontiers, CiRA, Kyoto University, 53 Shogoin Kawahara-cho, Sakyo-ku, Kyoto 606-8501, Japan
[7]Research Center for Stem Cell Engineering, National Institute of Advanced Industrial Science and Technology (AIST), 1-1-1 Higashi, Tsukuba, Ibaraki 305-8561, Japan
[8]Department of Immunogenetics, Graduate School of Medical Sciences, Kumamoto University, 1-1-1 Honjo, Chuo-ku, Kumamoto 860-8556, Japan
[9]Department of Cellular Oncology, Nagoya University Graduate School of Medicine, 65, Tsurumai-cho, Showa-ku, Nagoya 464-8603, Japan
[10]National Hospital Organization Nagoya Medical Center, 4-1-1, Sannomaru, Naka-ku, Nagoya 460-0001, Japan
*Correspondence: yuemura@east.ncc.go.jp (Y.U.), kaneko.shin@cira.kyoto-u.ac.jp (S.K.)
https://doi.org/10.1016/j.stemcr.2018.04.025

SUMMARY

$CD4^+$ T helper (Th) cell activation is essential for inducing cytotoxic T lymphocyte (CTL) responses against malignancy. We reprogrammed a Th clone specific for chronic myelogenous leukemia (CML)-derived b3a2 peptide to pluripotency and re-differentiated the cells into original TCR-expressing T-lineage cells (iPS-T cells) with gene expression patterns resembling those of group 1 innate lymphoid cells. CD4 gene transduction into iPS-T cells enhanced b3a2 peptide-specific responses via b3a2 peptide-specific TCR. iPS-T cells upregulated CD40 ligand (CD40L) expression in response to interleukin-2 and interleukin-15. In the presence of Wilms tumor 1 (WT1) peptide, antigen-specific dendritic cells (DCs) conditioned by CD4-modified $CD40L^{high}$ iPS-T cells stimulated WT1-specific CTL priming, which eliminated WT1 peptide-expressing CML cells *in vitro* and *in vivo*. Thus, CD4 modification of $CD40L^{high}$ iPS-T cells generates innate lymphoid helper-like cells inducing bcr-abl-specific TCR signaling that mediates effectiveanti-leukemic CTL responses via DC maturation, showing potential for adjuvant immunotherapy against leukemia.

INTRODUCTION

Tumor antigen-specific $CD4^+$ T helper (Th) cells can induce a wide range of tumor antigen-specific cytotoxic T lymphocyte (CTL) responses via the maturation of dendritic cells (DCs), which avoid tumor evasion because of a mutation in a single target epitope (Kreiter et al., 2015). In addition, Th cells can attenuate the immunosuppressive properties of the tumor microenvironment by altering the cytokine milieu (Kim and Cantor, 2014). Therefore, adoptive T cell therapy using *ex vivo* expanded antigen-specific $CD4^+$ Th cells may be a promising therapeutic strategy for refractory malignant tumors including hematological malignancies. However, clinical application is limited by the difficult isolation of $CD4^+$ Th cells specific for relevant antigens and limited proliferative potential of these cells.

This problem may be solved by using induced pluripotent stem cell (iPSC) technology. We and others have reported methods for establishing iPSCs from mature antigen-specific T cells and re-differentiating the iPSCs into $CD8^+$ T cells or invariant T cells with the same T cell antigen receptor (TCR) as the original T cells (Kitayama et al., 2016; Nishimura et al., 2013; Vizcardo et al., 2013; Wakao et al., 2013). The proliferative potential of iPSCs may provide a sufficient number of $CD4^+$ Th cells for cancer treatment.

CD40 ligand (CD40L), which is expressed on activated $CD4^+$ Th cells, is critical for inducing DC maturation via the CD40-CD40L interaction (Bennett et al., 1997, 1998; Boise et al., 1995; Ridge et al., 1998; Schoenberger et al., 1998; Summers deLuca and Gommerman, 2012; Wiesel and Oxenius, 2012). Recently, the expression of CD40L on other types of immune cells known as innate lymphoid cells (ILCs) was reported (Magri et al., 2014; McKenzie et al., 2014; Summers deLuca and Gommerman, 2012). ILCs play a fundamental role in the immune system not only by initiating, regulating, and resolving inflammation, but also by modulating adaptive immunity (Sonnenberg and Artis, 2015). Although they lack TCRs, ILCs show T helper properties similar to Th1, Th2, Th17, and Th22 cells in terms of their cytokine profiles and transcription factors, which determine their development (McKenzie et al., 2014). The contribution of ILCs to pathogen control and pathogenesis,

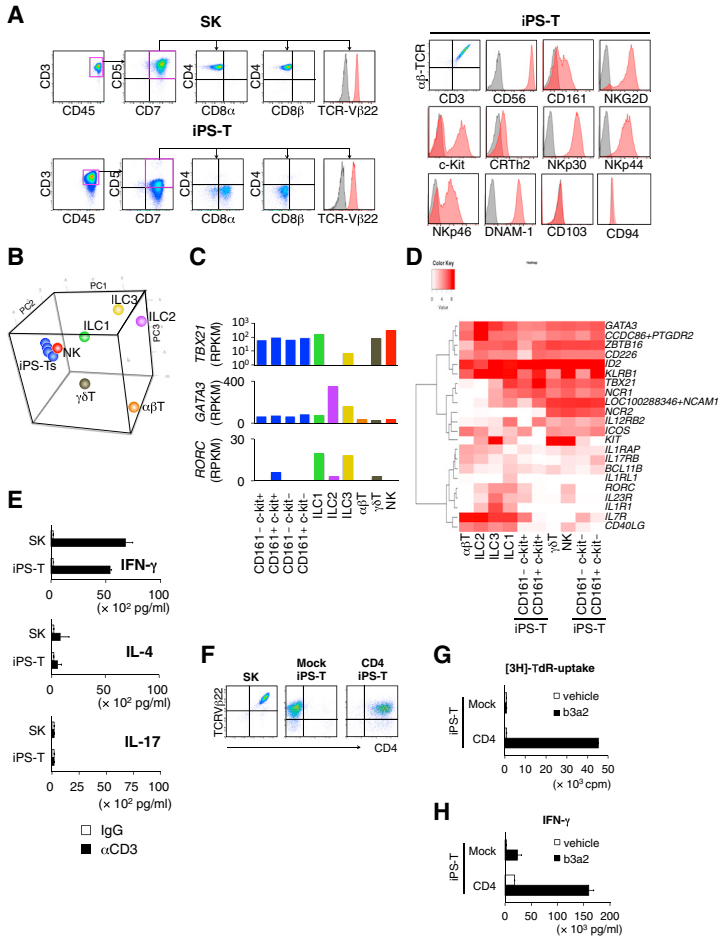

Figure 1. Re-differentiation and CD4 Modification of T-Lineage Cells from CD4⁺ Th1 Clone-Derived iPSCs Exert HLA Class II-Restricted Responses

(A) Representative flow cytometry profiles of the indicated molecules on the original CD4+ Th clone (SK) and regenerated T cells (iPS-T cells) after 14 days of phytohemagglutinin (PHA)-P stimulation.

(B) Principal component analysis of expression profiles of 146 selected T cell/ILC-related genes (Table S3).

(C) *GATA3*, *RORC*, and *TBX21* expression in the indicated population. mRNA expression levels were determined by RNA sequencing.

(D) Hierarchical clustering of expressions of 22 selected genes related to ILC subsets.

(E) Cytokine production of the original CD4⁺ Th1 clone (SK) and iPS-T cells. T cells were stimulated with plate-bound control immunoglobulin (immunoglobulin G [IgG]) or anti-CD3 mAb (10 μg/mL) for 24 hr. The indicated cytokines in the culture supernatant were measured by ELISA. Data shown are the means ± SD of triplicate cultures and are representative of two independent experiments.

(F) Representative flow cytometry profiles of CD4 and TCR-Vβ22 expression on the original CD4+ Th1 clone (SK), Mock transduced iPS-T cells (Mock iPS-T cells), and CD4-transduced iPS-T cells (CD4⁺ iPS-T cells).

(G) Proliferative responses of Mock iPS-T cells and CD4⁺ iPS-T cells to antigenic peptide. T cells were co-cultured with autologous PBMCs in the presence of b3a2 peptide (10 μM) and measured by the [³H]thymidine incorporation assay. Data shown are the means and are representative of two independent triplicate experiments.

(H) b3a2 peptide-specific IFN-γ production by Mock iPS-T cells and CD4+ iPS-T cells. Mock iPS-T cells and CD4+ iPS-T cells (1×10^5) were co-cultured for 24 hr with autologous DCs (5×10^4) that had been prepulsed with b3a2 peptide (10 μM). IFN-γ in the culture supernatant (24 hr) was measured by ELISA. Data shown are the means ± SD of triplicate cultures and are representative of two independent experiments.

along with their similarity and redundancy to acquired immune cells, are current of interest in immunology research (Cording et al., 2016).

In the present study, we established iPSCs from a CD4⁺ Th1 clone specific for the junction region of BCR-ABL p210 (b3a2), a leukemia antigen, which is restricted by HLA class II (HLA-DR9) (Ueda et al., 2016). We induced re-differentiation of iPSCs to T-lineage cells expressing HLA class II-restricted TCR (iPS-T cells). The gene expression profile of iPS-T cells differed from that of αβTCR⁺ T cells and resembled a subset of ILCs. By transferring CD4 molecule to iPS-T cells and optimizing the *ex vivo* culture conditions to induce iPS-T cells with high CD40L expression, we successfully generated innate lymphoid helper-like cells that activated leukemic antigen-specific CTLs via DC maturation in a TCR-dependent antigen-specific manner. The activated CTLs showed effective anti-leukemic activity.

Our findings indicate that functional helper-like cells can be acquired from iPS-T cells through genetic modification and purification of the population. Therefore, $CD40L^{high}$ CD4⁺ iPS-T cells are a potential platform for novel adjuvant cell therapy against malignant tumors.

RESULTS

ILC-like Properties of T-Lineage Cells Differentiated from CD4⁺ Th1 Clone-Derived iPSCs

We previously established an HLA-DR9-restricted leukemia antigen (b3a2)-specific CD4⁺ Th1 clone (SK). Using our T cell regeneration protocol with slight modifications (Figure S2A), we obtained CD3⁺ CD45⁺ $CD5^{dim+}$ CD7⁺ $CD8\alpha^{dim+}$ $CD8\beta^{-}$ cells from CD4⁺ Th1 clone (SK)-derived iPSCs (Figure 1A, left panel). The cells did not express CD4 throughout cell processing and heterogeneously

expressed several ILC markers including CD56, CD161, NKG2D, c-Kit, NKp30, NKp44, NKp46, and DNAM-1 (Figure 1A, right panel). Despite their heterogeneity, the cells consistently expressed the same TCR as the original CD4$^+$ Th1 clone (SK) (Figure S2B). Based on the expression of CD161 and c-Kit, iPS-T cells were divided into four subpopulations (Figure S2C), and their global RNA expression patterns were compared with those of natural killer (NK) cells, type 1 ILCs (ILC1s), type 2 ILCs (ILC2s), type 3 ILCs (ILC3s), αβT cells, and γδT cells isolated from peripheral blood (Figure S2D). iPS-T cells had genetic properties more consistent with those of ILC1s, NK cells, and γδT cells than those of peripheral αβT cells (Figure S2E; Table S2). The expression of genes related to T cell and ILC functions in iPS-T cells were similar to those in NK cells or ILC1s (Figures 1B and S2F; Table S3). Gene ontology and Kyoto Encyclopedia of Genes and Genomes pathway analysis revealed enrichment of genes related to "NK cell-related cytotoxicity" in iPS-T cells, NK cells, and ILC1s (Table S4). All subpopulations of iPS-T cells expressed relatively low levels of *BCL11B*, an essential transcription factor for T cell differentiation, compared with αβT cells, but relatively high levels of *ID2* and *ZBTB16*, which are transcription factors for ILCs (Figures S2G and S4F) (Naito et al., 2011; Spits et al., 2013). All subpopulations commonly expressed ILC1-related genes, such as *NCAM1*, *NCR1*, *NCR2*, *ICOS*, and *IL12RB2*, but low levels of *IL7R* and *IL1R*, which are expressed on all ILCs except NK cells (Figure 1D) (Spits et al., 2013). The ILC1/NK-like genetic properties of iPS-T cells, indicated by the relatively high expression of *TBX21* and relatively low expression of *GATA3* and *RORC*, were confirmed by the reads per kilobase million value and qRT-PCR analysis (Figure 1C, and data not shown). As reported previously, our iPS-T cells exhibited TCR-independent NK cell-like cytotoxicity (Figure S2H) (Kitayama et al., 2016; Yamada et al., 2016). The iPS-T cells produced high levels of interferon-γ (IFN-γ), comparatively low levels of interleukin-4 (IL-4), and no IL-17, which are similar to the original CD4$^+$ Th1 clone (SK) (Figure 1E). In addition, iPS-T cells were expanded by up to several thousand-fold by two rounds of phytohemagglutinin (PHA)-P stimulation (Figure S2I). These data suggest that iPS-T cells generated from the CD4$^+$ Th1 clone have group 1 ILC-like properties despite their expression of TCR.

CD4 Modification Augments b3a2-Specific Responses in iPSC-Derived T Cells

During T cell activation, the binding of CD4 to HLA class II increases TCR signaling 30- to 300-fold (Janeway, 1992), suggesting that CD4 is essential for the complete activation of Th cells. Because our iPS-T cells expressed HLA class II-restricted TCR from the original CD4$^+$ Th1 clone (SK), we hypothesized that transduction of the CD4 gene in iPS-T cells results in enhanced TCR-dependent responses by peptide stimulation. We transduced the CD4 gene using a retroviral vector (Figure 1F). CD4-transduced iPS-T cells (CD4$^+$ iPS-T cells) showed an antigen-dependent proliferative response and cytokine production restricted by HLA-DR9 (Figures 1G, 1H, and S3A), which was consistent with the response of the original CD4$^+$ Th1 clone (SK) (Figures S3B–S3D). In contrast, iPS-T cells without CD4 transduction (Mock iPS-T cells) showed impaired proliferation and IFN-γ production (Figures 1G and 1H). Moreover, we confirmed that the acquired functions of CD4$^+$ iPS-T cells did not depend on the specific positional effect of integrated retroviral vectors (Figure S3E). The effect of CD4 modification was also validated in iPS-T cells derived from an HLA-DR53-restricted $GAD65_{113\text{-}131}$ peptide-specific CD4$^+$ Th clone (SA32.5) (Figures S4A–S4E) (Tabata et al., 1998). Next, we analyzed the global gene expression profiles of Mock iPS-T cells and CD4$^+$ iPS-T cells stimulated with b3a2 peptide- or vehicle-loaded THP-1-expressing HLA-DR9 (THP-1-DR9) cells. The gene expression profile of CD4$^+$ iPS-T cells stimulated by b3a2 peptide differed from that of cells without b3a2 peptide and/or CD4 transduction (Figures S5A and S5B, Table S5). Gene ontology analysis revealed that categories related to cell proliferation were significantly upregulated in b3a2-stimulated CD4$^+$ iPS-T cells compared with b3a2-stimulated Mock iPS-T cells (Figure S5C). These data collectively indicate that CD4 gene modification gives iPS-T cells an enhanced ability to exert b3a2 peptide-specific and HLA class II-restricted responses.

Identification of a CD40L^{high} Population that Efficiently Exerts Adjuvant Function

CD40L expression on activated CD4$^+$ Th cells is critical for the maturation of DCs, which provide costimulatory signals for effective activation and enhanced survival of antigen-specific CD8$^+$ T cells (Bennett et al., 1997, 1998; Boise et al., 1995; Ridge et al., 1998; Schoenberger et al., 1998; Wiesel and Oxenius, 2012). In addition to CD4$^+$ Th cells, IL-7 plus IL-1β primed murine ILC3 cells (Magri et al., 2014) and IL-2-activated human NK cells (Carbone et al., 1997) were reported to express functional levels of CD40L. We hypothesized that iPS-T cells express CD40L under stimulation by IL-2 receptor subunit γ (common γ chain), which binds to other ligand (IL-2, 4, 7, 9, 15, 21)-specific receptors. We detected preferential expression of *CD40LG* and simultaneous expression of partner cytokine receptors for common γ chain including *IL2RA*, *IL2RB*, *IL2RG*, and *IL15RA* in the c-Kit$^+$ CD161$^+$ subpopulation (Figure S5D and data not shown). We cultured iPS-T cells in several combinations of common γ chain cytokines and found that IL-2 in combination with IL-15 upregulated CD40L expression (Figures 2A and 2B).

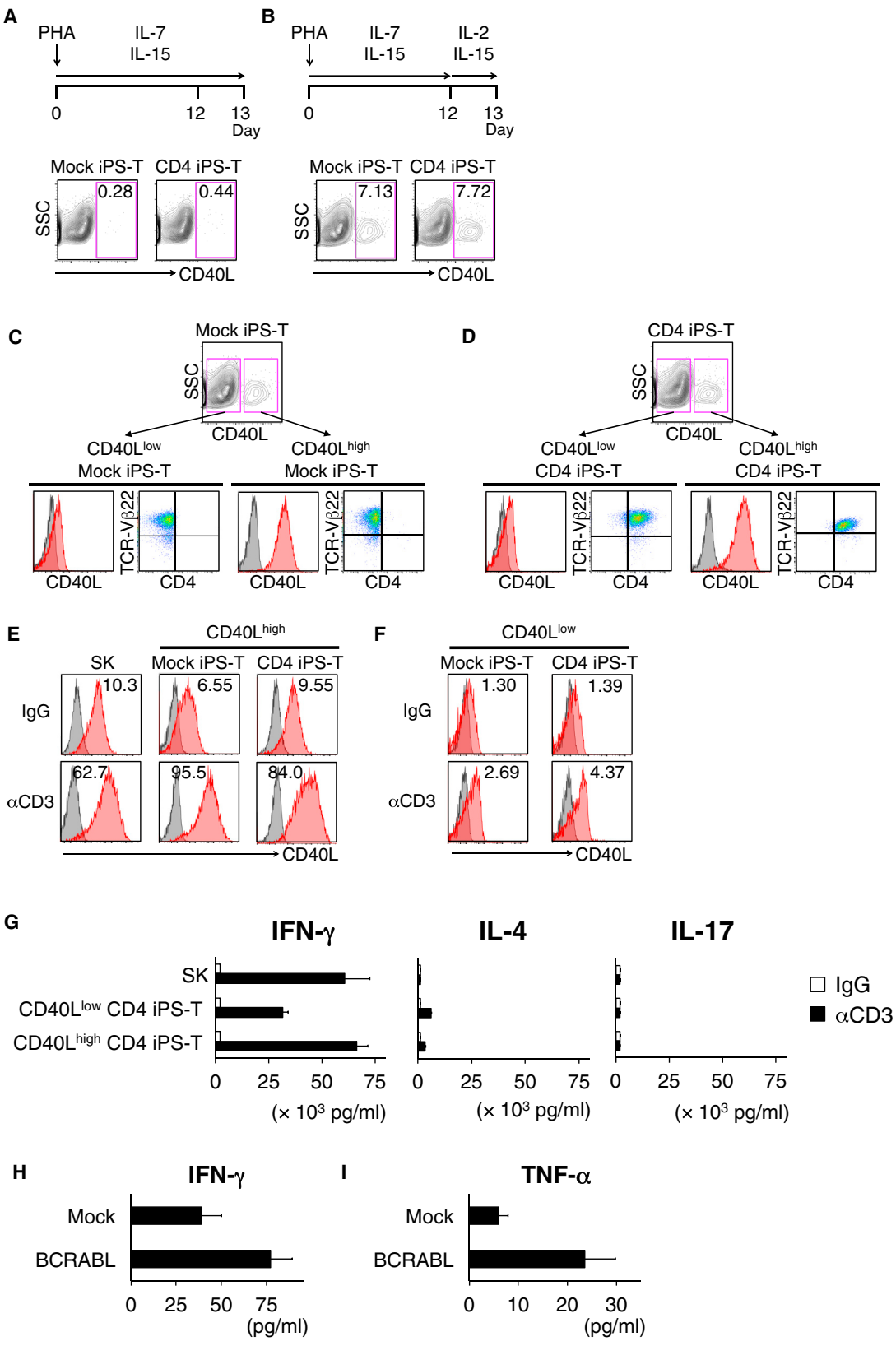

(legend on next page)

The IL-2/IL-15-induced CD40L^{high} and CD40L^{low} populations were separated and expanded by PHA-P stimulation. Each CD40L^{high} and CD40L^{low} population from Mock iPS-T cells and CD4$^+$ iPS-T cells expressed TCR-Vβ22 and retained their CD40L expression levels in the presence of IL-2 and IL-15 (Figures 2C and 2D). Upon stimulation with an anti-CD3 antibody, only CD40L^{high} iPS-T cells showed upregulated CD40L expression (Figures 2E and 2F). CD40L^{high} CD4$^+$ iPS-T cells produced higher levels of IFN-γ and tumor necrosis factor alpha (TNF-α) than did CD40L^{low} CD4$^+$ iPS-T cells, but the two populations consistently produced low levels of IL-2, IL-4, IL-6, IL-10, and IL-17 (Figures 2G and S6A). When stimulated with b3a2-peptide-loaded DCs, co-expression of CD4 and CD40L synergistically enhanced the production of IFN-γ and TNF-α, indicating a Th1-biased cytokine profile (Figure S6B). In addition, when CD40L^{high} CD4$^+$ iPS-T cells were co-cultured with THP-1-DR9 cells expressing BCR-ABL p210 protein, they produced IFN-γ and TNF-α, indicating their ability to respond to the naturally processed BCR-ABL p210 epitope (Figures 2H and 2I). CD40L^{high} CD4$^+$ iPS-T cells can expand against repeated stimulation without affecting CD3, CD5^{dim}, CD7, and CD8α expression (Figures S6C and S6D). Similar findings associated with CD40L expression were obtained in iPS-T cells from an HLA-DR53-restricted GAD65$_{113\text{-}131}$ peptide-specific CD4$^+$ Th clone (SA32.5) (Figures S7A–S7E). Collectively, we identified a population of CD4$^+$ iPS-T cells with upregulated CD40L expression in response to TCR stimulation and possessed a superior ability to respond to antigenic peptide stimulation.

Next, we analyzed the cellular adjuvant function of CD4$^+$ iPS-T cells to induce DC maturation. When CD40L^{high} CD4$^+$ iPS-T cells were co-cultured with immature DCs pre-pulsed with b3a2 peptide, they induced maturation of DCs (Figures 3A and S7F). In contrast, DC maturation by CD40L^{low} CD4$^+$ iPS-T cells was impaired (Figures 3A and S7F). Furthermore, CD40L^{low} Mock iPS-T cells failed to induce DC maturation, possibly via impaired recognition of the HLA class II/peptide complex because of the absence of CD4 (Figures 3A and S7F). CD40L^{high} CD4$^+$ iPS-T cells also enhanced the production of IL-12p70, CXCL9, and CXCL11, which are important soluble factors in the activation and migration of NK cells, Th1 cells, and CTLs (Figure 3B). These data indicate that CD40L^{high} CD4$^+$ iPS-T cells have a superior ability to induce DC maturation.

It was previously reported that the CD40L-CD40-mediated ILC3-B cell interactions induce regulatory B cells to secrete the T cell-suppressing cytokine IL-10 (Komlosi et al., 2017); thus, we examined whether CD40L^{high} CD4$^+$ iPS-T cells induce the immune inhibitory cytokine IL-10 by interacting with DCs or B cells. Both CD40L^{high}- and CD40L^{low}-CD4$^+$ iPS-T cells alone did not produce IL-10 upon CD3 stimulation (Figure S6A). When DCs or B cells were co-cultured with CD40L^{high} CD4$^+$ iPS-T cells in the presence of the b3a2 peptide, they did not produce IL-10, whereas DCs co-cultured with CD40L^{low} CD4$^+$ iPS-T cells produced IL-10 (Figure S7G). These data indicate that CD40L^{high} CD4$^+$ iPS-T cells do not stimulate IL-10 production, which is an appropriate property for eliciting anti-leukemic immune responses.

CD40L^{high} CD4$^+$ iPSC-Derived T Cells Reduced TCR-Independent Cytotoxicity

CD4$^+$ Th1 clone (SK)-derived iPS-T cells exhibited antigen-independent cytotoxicity against THP-1, and the cytotoxicity against THP-1 was partially dependent on perforin and DNAM-1 (Figure 4A). iPS-T cells exert DNAM-1- and NKG2D-dependent cytotoxicity against K562 cells expressing both DNAM-1 ligand (PVR, nectin-2) and NKG2D ligands (MICA/B) (Kitayama et al., 2016). Despite the expression of both NK receptors, the iPS-T cells used in this study did not show NKG2D-dependent cytotoxicity (Figure 4A). This may be because of the reduced expression of NKG2D ligands (MICA/B) on THP-1 target cells (Figure S7H). CD40L^{high} CD4$^+$ iPS-T cells conditioned by IL-2/IL-15

Figure 2. CD40L^{high} Population in iPS-T Cells Shows High Responsiveness to TCR Stimulation

(A and B) CD40L expression of indicated iPS-T cells on day 13 after PHA-P stimulation. Mock iPS-T cells or CD4$^+$ iPS-T cells were stimulated with PHA-P and cultured in the absence (A) or presence (B) of IL-2. The frequency of CD40L-positive cells is shown in the upper right corner of each panel.

(C and D) Expression of CD40L, CD4, and TCR-Vβ22 on the subpopulations are shown. CD40L high and low populations under IL-2 (100 U/mL) and IL-15 (5 ng/mL) were separated from Mock iPS-T cells (C) and CD4$^+$ iPS-T cells (D) by flow cytometry sorting and expanded by PHA-P stimulation.

(E and F) Surface CD40L expression on different subpopulations (E; CD40L high and F; CD40L low) stimulated with plate-bound control IgG or anti-CD3 mAb (10 μg/mL). The original CD4$^+$ Th1 clone (SK) served as a control. CD40L (red) and isotype-matched controls (gray) are shown.

(G) Cytokine production by the indicated population stimulated with plate-bound control IgG or anti-CD3 mAb (10 μg/mL). The original CD4$^+$ Th1 clone (SK) served as control. (H) Cytokine production by CD40L^{high} CD4$^+$ iPS-T cells (1×10^5) co-cultured with THP1 cells (5×10^4) expressing HLA-DR9 and BCR-ABL p210 gene. (G and H) The indicated cytokines in the culture supernatant (24 h) were measured by a bead-based multiplex immunoassay. Data shown are the means ± SD of triplicate cultures and are representative of two independent triplicate experiments.

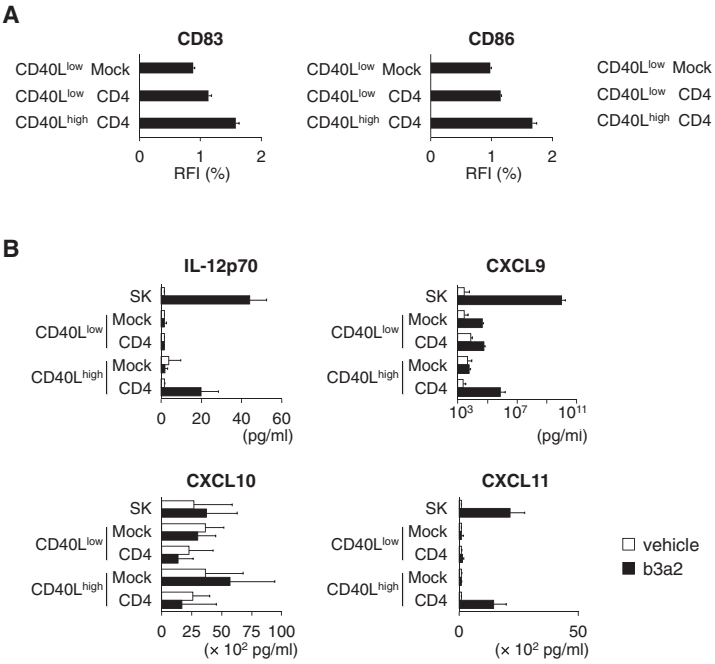

Figure 3. DC Activation Induced by CD40L^{high} CD4$^+$ iPS-T Cells

(A) Flow cytometry profiles of the surface molecules on DCs. Vehicle- or b3a2-peptide-pulsed DCs were cultured for 24 hr with the CD40L^{high} CD4$^+$ and CD40L^{low} CD4$^+$ population at a DC/CD4$^+$ iPS-T cell ratio of 5:1. Relative fluorescence intensity (RFI) (%) of indicated molecule is calculated as follows: RFI (%) = 100 × (RFI of b3a2 peptide-treated cells)/(RFI of vehicle-treated cells).

(B) Cytokine production by DCs co-cultured with the indicated population. Cytokines in the culture supernatant were measured by a bead-based multiplex immunoassay. The indicated population (1×10^4) was co-cultured for 24 hr with autologous DCs (2.5×10^4) that had been prepulsed with b3a2 peptide (10 μM). The original CD4$^+$ Th1 clone (SK) served as a control.

(A and B) Data shown are the means ± SD of triplicate cultures and are representative of two independent experiments.

exhibited reduced expression of DNAM-1 and NKG2D compared with CD40L^{low} CD4$^+$ iPS-T cells (Figure 4B, left panel). Consistent with the reduced DNAM-1 and NKG2D expression, CD40L^{high} CD4$^+$ iPS-T cells reduced NK cell-like cytotoxicity against THP-1-DR9 while retaining b3a2-specific cytotoxicity (Figure 4B, right panel). These data indicate that CD40L^{high} CD4$^+$ iPS-T cells reduced antigen-independent cytotoxicity by downregulating DNAM-1 expression.

CD40L^{high} CD4$^+$ iPSC-Derived T Cells Efficiently Induce Primary Expansion of Leukemia Ag-Specific CTLs

CD4$^+$ Th cells help in the priming of CD8$^+$ CTLs via DC activation (Bennett et al., 1997; Ridge et al., 1998; Schoenberger et al., 1998; Ueda et al., 2016). To determine whether CD40L^{high} CD4$^+$ iPS-T cells can induce leukemia antigen-specific CTL responses, vehicle- or b3a2 peptide-loaded DCs were cultured with CD40L^{high} CD4$^+$ iPS-T cells, and differentially conditioned DCs were loaded with Wilms tumor 1 ($WT1_{235-243}$) peptide, irradiated, and cultured with CD8$^+$ T cells (Figure S8A). After 7 days of culture, the proliferation of CD8$^+$ T cells was evaluated. We observed markedly enhanced proliferation of CD8$^+$ T cells upon stimulation with $WT1_{235-243}$ peptide when CD40L^{high} CD4$^+$ iPS-T cell/b3a2 peptide-conditioned DCs were used as antigen-presenting cells (Figure 5A, left panel). In contrast, neither CD40L^{low} CD4$^+$ iPS-T cell/b3a2-conditioned DCs nor CD40L^{low} Mock iPS-T cell/b3a2-conditioned DCs induced the proliferation of CD8$^+$ T cells (Figure 5A, center and right panel). CTLs stimulated by CD40L^{high} CD4$^+$ iPS-T cell/b3a2 peptide-conditioned DCs contained a high frequency of WT1-tetramer-positive T cells (Figure 5B, left panel). WT1 peptide-specific CTLs were further expanded by repeated stimulation with WT1 peptide three times (Figure 5B, center panel). The expanded WT1-specific CTLs exhibited cytotoxic activity against WT1 peptide-loaded HLA-A24-expressing K562, but not against vehicle-loaded cells (Figure 5B, right panel). These data indicate that the activation of CD40L^{high} CD4$^+$ iPS-T cells by the b3a2 peptide induces DC-mediated cellular adjuvant properties that can increase leukemic antigen-specific CTL responses, which is consistent with the T helper function of the original CD4$^+$ Th1 clone (SK) (Ueda et al., 2016).

WT1-Specific CTLs Primed By CD40L^{high} CD4$^+$ iPSC-Derived T Cell/DC Interaction Exert Anti-leukemic Effects *In Vivo*

To examine whether primed WT1 peptide-specific CTLs exert anti-leukemic effects *in vivo*, WT1 epitope-expressing K562 cells were subcutaneously injected into NSG mice with or without WT1 peptide-specific CTLs. Tumor growth was monitored each week by bioluminescence imaging and external caliper measurements. In the presence of WT1 peptide-specific CTLs, tumor growth was significantly inhibited (Figure 6A) and the survival of mice was significantly prolonged (Figure 6B). Collectively, leukemic antigen-specific CTLs primed by the interaction of CD40L^{high} CD4$^+$ iPS-T cells and DCs exert effective anti-leukemic effects.

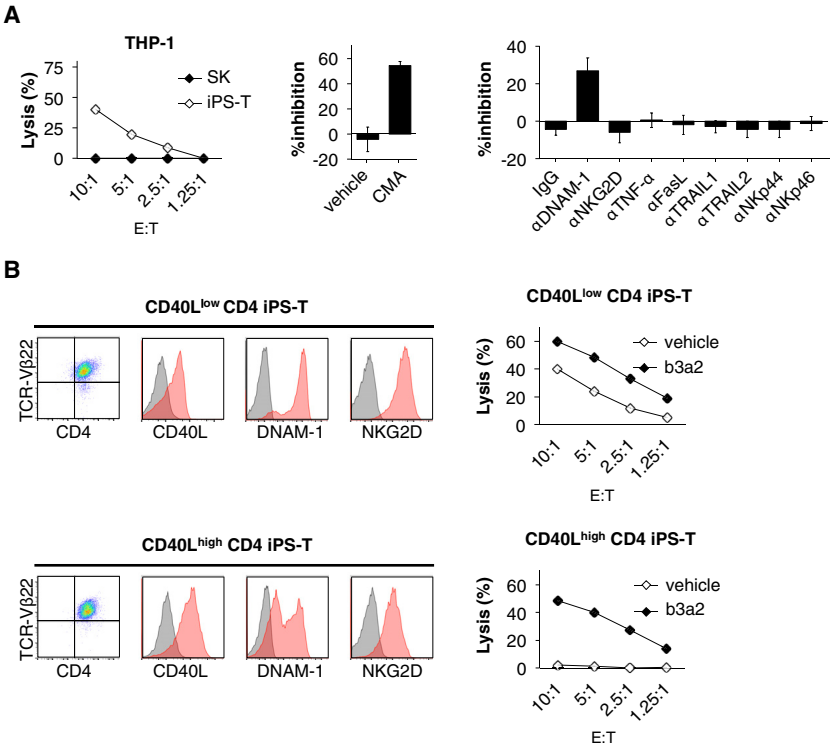

Figure 4. CD40L^{high} CD4^{+} iPS-T Cells Reduced NK Cell-like Cytotoxicity

(A) Left panel: cytotoxic activity of iPS-T cells to THP-1 cells. Center panel: Mock iPS-T cells were treated with 10 nM concanamycin A (CMA) to block perforin. Right panel: Indicated Abs blocking receptor/ligand interactions were added. Cytotoxicity of iPS-T cells to THP-1 cells at an effector/target (E:T) ratio of 2.5:1.

(B) Left panel: representative flow cytometry profiles of TCR-Vβ22, CD4, CD40L, DNAM-1, and NKG2D on the indicated population. Right panel: cytotoxic activities of the indicated population to HLA-DR9-expressing THP-1 cells loaded with vehicle or b3a2 peptide (5 μM).

(A and B) Cytotoxicity was measured by ^{51}Cr-release assay for 4 hr at the indicated E:T ratios. Data are representative of two independent triplicate experiments.

DISCUSSION

Although tumor antigen-specific CD4^{+} Th cells are essential for inducing downstream activation of diverse tumor antigen-specific CTLs, it is difficult to obtain clinically sufficient numbers of Th cells for adoptive cell therapy. The unlimited supply of Th cells from iPSCs may resolve this issue. To date, studies have not reported the successful generation of HLA class II-restricted CD4^{+} Th cells from iPSCs. We established iPSCs from b3a2-specific CD4^{+} Th cells (SK) and induced T-lineage cells (iPS-T cells) from these cells. Using the current differentiation protocol, the iPS-T cells spontaneously failed to express CD4 molecules, and their gene expression profiles were closer to those of ILC1s/NK cells than to those of αβT cells, which may be partially explained by insufficient control of the transcription factor BCL11B for specification to the T cell-lineage (Kitayama et al., 2016). Bcl11b insufficiency is known to cause biased lineage-reprogramming from T cells to NK cells (a lineage of type 1 ILCs) in conditional knockout mice (Li et al., 2010). Our iPS-T cells from multiple donors expressed ID2 and ZBTB16, but not BCL11B (Figure S4F). These features may partially explain the lineage-shift from T cells to type 1 ILCs during *in vitro* differentiation.

Modification of CD4 expression in the regenerated cells and purification of the CD40L^{high} population were performed to acquire ILC1-like cells that can stimulate DCs, thereby, promoting leukemia antigen-specific CTL responses. Although the detailed mechanisms of this artificial TCR signaling in group 1 ILC-like T cells are presently not known, TCR ligation via antigenic peptide/HLA molecule complexes induced proliferation and cytokine production in a manner consistent with that in αβT cells.

The interaction between CD40L^{high} CD4^{+} iPS-T cells and DCs facilitates the production of chemokines to recruit CXCR3-expressing effector cells (Figure 3B). IFN-γ production from these recruited effector cells activates DCs to amplify the production of chemokines (Groom and Luster, 2011). This positive feedback loop pathway may further facilitate the recruitment and activation of effector cells in tumor tissues. In the actual leukemia environment, CD40L^{high} CD4^{+} iPS-T cells may condition DCs to take up leukemia cells and cross-present leukemia-derived antigens, resulting in the activation of diverse CTLs that specifically recognize multiple leukemia antigens, a phenomenon known as epitope spreading. Chronic myelogenous leukemia (CML) cells carry a number of well-defined leukemia antigens including BCR-ABL, PR1, and WT1 (Molldrem et al., 2000; Rezvani et al., 2003). Moreover, TKI treatment of CML induces various mutations in the BCR-ABL kinase domain because of resistance. The mutated antigens may then generate highly immunogenic neoepitopes (Cai et al., 2012), and these neoepitopes are potential targets of epitope spreading by CD40L^{high} CD4^{+} iPS-T cells.

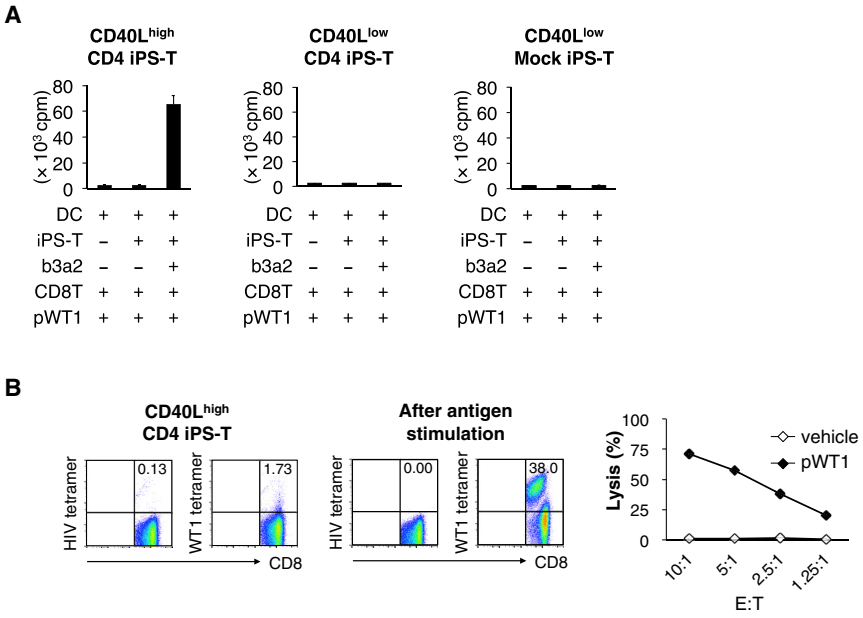

Figure 5. Induction of Leukemia Antigen-Specific CTLs By CD40L^{high} CD4$^+$ iPS-T Cells

(A) Proliferative response of CD8$^+$ T cells. Indicated iPS-T cells (5 × 10^3) and DCs (1 × 10^4) ± b3a2 peptide (5 μM) were initially co-cultured for 5 hr to mature the DCs, after which DCs and iPS-T cells were irradiated and cultured with autologous CD8$^+$ T cells (5 × 10^4) in the presence of WT1 peptide (5 μM). The proliferative response (day 7) was measured as the amount of [^{3}H]thymidine incorporated. Data shown are the means ± SD of triplicate cultures and are representative of two independent experiments.

(B) Left panels: frequency of WT1/HLA-A24 tetramer-positive CD8$^+$ T cells primed by CD40L^{high} CD4$^+$ iPS-T cell-conditioned DCs. CD40L^{high} CD4$^+$ iPS-T cells (5 × 10^3) and DCs (1 × 10^4) prepulsed with b3a2 peptide (5 μM) were initially co-cultured for 5 hr to mature the DCs, after which DCs and CD4$^+$ iPS-T cells were irradiated and cultured with autologous CD8$^+$ T cells (5 × 10^4) in the presence of WT1 peptide (5 μM). Tetramer staining at day 10 after stimulation is shown. Center panel: frequency of WT1/HLA-A24 tetramer-positive CD8$^+$ T cells after a third stimulation with WT1 peptide. Representative flow cytometry profiles of two independent experiments. HIV-env/HLA-A24 tetramer was used as a control. Right panel: cytotoxic activities of expanded WT1-specific CD8$^+$ T cells against K562-A24 loaded with vehicle or WT1 peptide. Cytotoxicity was measured by ^{51}Cr-release assay for 4 hr at the indicated E:T ratios. Data are representative of two independent triplicate experiments.

However, few suitable animal models are available that reproduce general reactions of human immune cells, particularly in HLA class II-restricted helper T cell/DC-mediated CTL priming and subsequent tumor elimination. Animal models reconstituted with the human hematopoietic system, immune system, tumor xenograft, and iPS-T cells derived from the same patient may overcome this limitation in the future.

Our study is an initial step toward clinically applicable iPSC-derived T helper-like cell therapy. However, iPSC-based regenerative medicine is accompanied by challenges, such as the fact that these strategies are time-consuming and expensive. Compared with an autologous setting, the use of HLA-matched or homozygous HLA-type allogeneic iPSCs transduced with desired TCR (i.e., obtained TCR sequences from this research) may resolve this issue in the preparation of CD40L^{high} CD4$^+$ iPS-T cells (Neofytou et al., 2015). In addition, reproducible production of CD4-expressing iPS-T cells is a prerequisite for their clinical application. In this study, CD4 gene transduction was performed after re-differentiation of iPSCs to T-lineage cells. Genome editing of iPSCs enables targeted insertion of the CD4 transgene into the downstream region of T cell-specific promoters, such as Lck promoter. Using such a system, it may be possible to establish an ideal iPSC clone expressing transgenes only at an ideal differentiation step when the promoter is activated. This may provide reproducible CD4-expressing iPS-T cells with safe profiles for clinical use. Moreover, establishing a good manufacturing practice-compliant manufacturing protocol using xenogeneic-free and feeder cell-free material is essential and currently under development (Fransen et al., 2011; Neofytou et al., 2015).

In conclusion, we showed that iPS-T cells from CD4$^+$ Th clone-derived iPSCs constitute a heterogeneous population of TCR-expressing group 1 ILC-like lymphoid cells. Gene modification and cell purification resulted in the acquisition of HLA class II-restricted TCR-expressing adjuvant cells that induce anti-leukemia effects via DC maturation. These results support iPS-T cells as a potential platform for novel adjuvant therapy for leukemia.

EXPERIMENTAL PROCEDURES

Peptide, Cytokines, and Chemicals

HLA-DR9 (DRB1*09:01)-restricted BCR-ABL b3a2-junctional peptide (ATGFKQSSKALQRPVAS), HLA-A24 (A*24:02)-restricted modified WT1$_{235–243}$ epitope peptide (CYTWNQMNL), and HLA-DR53 (DRB4*01:03)-restricted glutamic acid decarboxylase 65 (GAD65)$_{113-131}$ peptide (DVMNILLQYVVKSFDRSTK) were commercially synthesized and supplied at >90% purity (Toray Research Center, Kamakura, Japan, Scrum, Tokyo, Japan). In the modified WT1$_{235-243}$ peptide, Y was substituted for M at amino acid position 2 of the natural WT1$_{235-243}$ peptide (CYTWNQMNL).

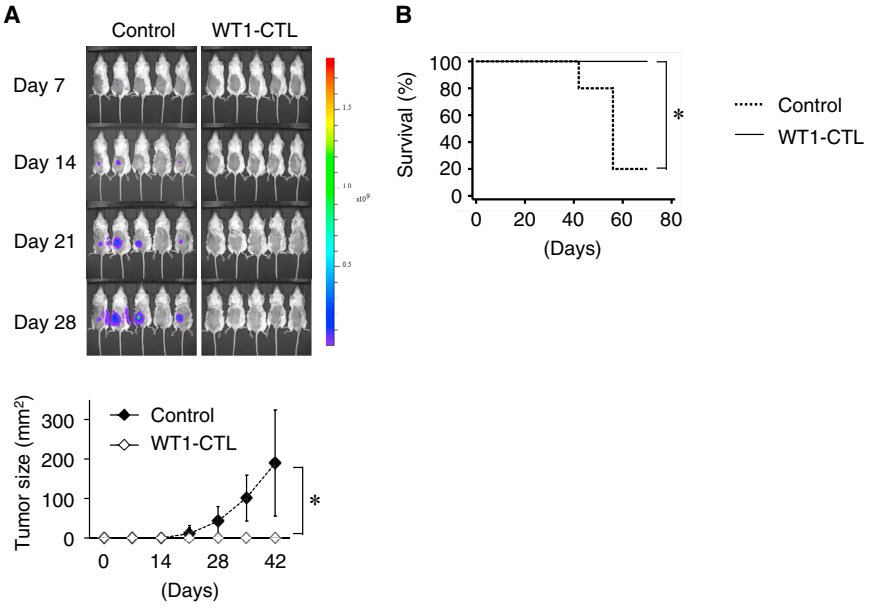

Figure 6. Anti-leukemic Activity of CTLs Primed By CD40L^{high} CD4^{+} iPS-T Cell-Conditioned DCs

(A) *In vivo* anti-leukemia effect. NSG mice were subcutaneously injected with mixtures of K562-A24-Luc-WT1 minigene and either saline or WT1-specific CTLs. Upper panel: tumor burden was measured weekly by bioluminescence imaging. Lower panel: the average tumor size for each group from day 0 to 42 is shown. Error bars represent ± SD. *$p < 0.05$ by unpaired Student's t test (two-tailed).

(B) Kaplan-Meier survival curves for treated and control mice. *$p < 0.05$ by the log rank (Mantel-Cox) test. WT1-CTL, n = 10; no treatment, n = 5.

The following reagents were from commercial sources: recombinant human (rh) IL-2, rhIL-4, and rh granulocyte macrophage colony-stimulating factor (Primmune, Osaka, Japan); rhIL-7, rhIL-15, and rh fms-related tyrosine kinase 3 ligand (Flt-3L) (PeproTech, Rocky Hill, NJ, USA); rh basic fibroblast growth factor and PHA-P (Wako Pure Chemicals Industries, Osaka, Japan); rh vascular endothelial growth factor and rh stem cell factor (R&D Systems, Minneapolis, MN, USA); and penicillin-killed *Streptococcus pyogenes* (OK432) (Chugai Pharmaceutical, Tokyo, Japan).

Generation of Retrovirus for CD4 Transduction

The human CD4 gene was inserted into pDON-AI2 (Takara Bio, Shiga, Japan). Transient retroviral particles were produced in G3T-hi cells (Takara Bio), followed by transduction of PG13 cells to generate GaLV-pseudotyped retrovirus producer cells (Kaneko et al., 2001).

Generation of iPSCs Derived from HLA Class II-Restricted Antigen-Specific CD4^{+} T Cell Clone

HLA-DR9-restricted b3a2-specific CD4^{+} Th1 clone (SK) (Ueda et al., 2016) and HLA-DR53-restricted GAD65$_{113\text{-}131}$ peptide-specific CD4^{+} Th clone (SA32.5) (Tabata et al., 1998) were reprogrammed to iPSCs by transduction of reprogramming factors by the Sendai viral system using pSeV[KOSM302L] (kindly provided by Dr. Nakanishi, AIST, Tsukuba, Japan) as described previously (Kitayama et al., 2016; Nishimura et al., 2013). The iPSC clones were negative for residual transgenes, showed pluripotency characterized by the expression of pluripotency-related molecules and teratoma formation in immunodeficient mice, and were confirmed to have a normal karyotype (Figure S1). The use of cells isolated from healthy adults was approved by the Ethics Committee of Kyoto University, and informed consent was obtained from all donors in accordance with the Declaration of Helsinki.

T Cell Differentiation from iPSCs and CD4 Transduction

We differentiated iPSCs into T cells using a previously described method (Nishimura et al., 2013). In brief, clumps of iPSCs were transferred onto C3H10T1/2 feeder cells and cultured in EB medium containing rh vascular endothelial growth factor. On day 7, rh stem cell factor and rhFlt-3L were added to the culture. On day 14, hematopoietic progenitor cells were collected and transferred onto OP9-DL1 cells and co-cultured in OP9 medium in the presence of rhIL-7 and rhFLT-3L. On day 35, regenerated T cells were stimulated by PHA-P in the presence of rhIL-7 and rhIL-15 using allogeneic peripheral blood mononuclear cells (PBMCs) as antigen-presenting cells at 14-day intervals. Expanded iPSC-T cells (1×10^6) were transduced with human CD4 using the RetroNectin-bound virus infection method, in which retroviral solution was preloaded onto RetroNectin-coated plates, centrifuged at 2,000 $\times g$ for 2 hr at 32°C, and rinsed with 1.5% human serum albumin PBS, after which the cells were applied to the virus-preloaded plate for 20 hr. After 10 days of culture, a CD4-positive population (15%–35% of total cells) was sorted by flow cytometry and restimulated for expansion.

Functional Assay of T Cells

Cell proliferation was evaluated by the [^{3}H]thymidine incorporation assay, as described previously (Zhang et al., 2015). Cytotoxic activity was measured using the ^{51}Cr-release assay, as described previously (Zhang et al., 2015). Cytokine levels in the culture supernatants were evaluated by ELISA (hIFN-γ: eBioscience, San Diego, CA, USA) or a bead-based multiplex immunoassay (BD Cytomertic Beads Array; BD Biosciences, Franklin Lakes, NJ, USA).

CTL Priming and Cytotoxicity Assays

CD8^{+} T cells and DCs were obtained from the same donor from whom the b3a2-specific T cell clone (SK) was established. The cells

were used to induce antigen-specific CTLs to avoid alloreactive responses. $CD8^+$ T cells were isolated from PBMCs by negative magnetic cell sorting using a $CD8^+$ T cell isolation kit (Miltenyi Biotec, Bergisch Gladbach, Germany). DCs were cultured for 3 hr in 96-well round plates in the presence or absence of b3a2 peptide, and then the original $CD4^+$ Th1 clone (SK) or re-differentiated SK was added to the culture and incubated for 5 hr. After irradiation at 30 Gy, $CD8^+$ T cells were added together with $WT1_{235–243}$ peptide. On day 7, we added 1 μCi of [^{3}H]thymidine to the cultures; after 16-hr incubation, we assessed the proliferative response of $CD8^+$ T cells in a [^{3}H]thymidine incorporation assay. Another experiment was performed in the same manner on day 10. The frequencies of WT1-peptide-specific CTLs were determined by staining with the HLA-A*2402/$WT1_{235–243}$ tetramer. We restimulated the resulting $CD8^+$ T cells with $WT1_{235–243}$ peptide in the presence of 35-Gy-irradiated autologous PBMCs. The cells were later used in cytotoxicity assays and *in vivo* experiments.

In Vivo Experiments

All *in vivo* animal studies were approved by the Animal Research Committee of Kyoto University. Six-week-old female NOD-SCID $IL2R\gamma c^{null}$ (NSG) mice were purchased from Charles River (Yokohama, Japan) and inoculated subcutaneously in the left shaved shank with mixtures of K562-Luc-A24-WT1 minigene (1.0×10^5) cells and either saline or WT1-specific CTLs (1.0×10^6). The mice were monitored for tumor growth and survival. Tumor growth was monitored weekly by bioluminescence imaging for 4 weeks and external caliper measurements until the mice died or were sacrificed when tumors exceeded 25 mm in diameter.

Retroviral Integration Site Analysis by Linear Amplification-Mediated PCR

Retroviral integration site analysis was performed using the Retro-X Integration Site Analysis Kit (Clontech, Mountain View, CA, USA) according to the manufacturer's instructions.

Statistical Analysis

STATA version 13.0 (StataCorp LP, College Station, TX, USA) was used for all statistical analyses. To compare multiple experimental groups, one-way ANOVA with Bonferroni *post hoc* test was used to assess significance; to compare two experimental groups, unpaired t tests (two-tailed) were used. For statistical analysis of Kaplan-Meier survival curves, a log rank (Mantel-Cox) test was used to calculate p values; p values < 0.05 were considered statistically significant and are indicated in the figures by asterisks.

SUPPLEMENTAL INFORMATION

Supplemental Information includes Supplemental Experimental Procedures, eight figures, and five tables and can be found with this article online at https://doi.org/10.1016/j.stemcr.2018.04.025.

AUTHOR CONTRIBUTIONS

N.U., Y.U., and S. Kaneko designed the study. N.U., R.Z., S. Kitayama, Y.Y., S.I., T.-Y.L., Y.M., C.O., A.W., S.S., Y.N., K.K., H.K., Y.U., and S. Kaneko interpreted the data. N.U., Y.U., R.Z., S. Kitayama, Y.Y., M.T., and Y.M. performed the experiments. M.N. provided critical materials. N.U., R.Z., Y.M., and A.W. analyzed the data. S.I., Y.K., T.U., T.-Y.L., S.S., K.K., Y.N., H.K., and T.N. contributed to analyzing and discussing the data. Y.U. and S. Kaneko supervised the study. N.U., Y.U., and S. Kaneko wrote the manuscript.

ACKNOWLEDGMENTS

CSII-EF, pCMV-VSV-G-RSV-Rev, and pCAG-HIVgp were kindly provided by Dr. H. Miyoshi (RIKEN BioResource Center, Tsukuba, Japan). cDNA encoding *HLA-DRB1*09:01* (*DR9*) was kindly provided by Dr. H. Kobayashi (Asahikawa Medical College, Asahikawa, Japan). We thank Dr. P. Karagiannis (Kyoto University, Kyoto, Japan) for reading the manuscript. This study was performed as a research program of the Project for Development of Innovative Research on Cancer Therapeutics (P-DIRECT) and Core Center for iPS Cell Research of Research Center Network for Realization of Regenerative Medicine, Japan Agency for Medical Research and Development. This study was supported by grants from Grants-in-Aid "Carcinogenic Spiral," Nagono Medical Foundation, the National Cancer Center Research and Development Fund (28-A-8) and the Takeda Science Foundation. Shin Kaneko is a founder, shareholder, and scientific advisor at Thya and received research funding from Kyowa Hakko Kirin, Takeda Pharmaceutical, Sumitomo Chemical, and Thyas. Hitoshi Kiyoi received research funding from Chugai Pharmaceutical, Bristol-Myers Squibb, Kyowa Hakko Kirin, Zenyaku Kogyo, FUJIFILM Corporation, Nippon Boehringer Ingelheim, Astellas Pharma, and Celgene Corporation, consulting fees from Astellas Pharma and Daiichi Sankyo, and honoraria from Bristol-Myers Squibb. The remaining authors declare no competing financial interests.

Received: October 10, 2017
Revised: April 27, 2018
Accepted: April 30, 2018
Published: May 24, 2018

REFERENCES

Bennett, S.R., Carbone, F.R., Karamalis, F., Flavell, R.A., Miller, J.F., and Heath, W.R. (1998). Help for cytotoxic-T-cell responses is mediated by CD40 signalling. Nature *393*, 478–480.

Bennett, S.R., Carbone, F.R., Karamalis, F., Miller, J.F., and Heath, W.R. (1997). Induction of a CD8+ cytotoxic T lymphocyte response by cross-priming requires cognate CD4+ T cell help. J. Exp. Med. *186*, 65–70.

Boise, L.H., Minn, A.J., Noel, P.J., June, C.H., Accavitti, M.A., Lindsten, T., and Thompson, C.B. (1995). CD28 costimulation can promote T cell survival by enhancing the expression of Bcl-XL. Immunity *3*, 87–98.

Cai, A., Keskin, D.B., DeLuca, D.S., Alonso, A., Zhang, W., Zhang, G.L., Hammond, N.N., Nardi, V., Stone, R.M., Neuberg, D., et al. (2012). Mutated BCR-ABL generates immunogenic T-cell epitopes in CML patients. Clin. Cancer Res. *18*, 5761–5772.

Carbone, E., Ruggiero, G., Terrazzano, G., Palomba, C., Manzo, C., Fontana, S., Spits, H., Karre, K., and Zappacosta, S. (1997). A new mechanism of NK cell cytotoxicity activation: the CD40-CD40 ligand interaction. J. Exp. Med. *185*, 2053–2060.

Cording, S., Medvedovic, J., Aychek, T., and Eberl, G. (2016). Innate lymphoid cells in defense, immunopathology and immunotherapy. Nat. Immunol *17*, 755–757.

Fransen, M.F., Sluijter, M., Morreau, H., Arens, R., and Melief, C.J. (2011). Local activation of CD8 T cells and systemic tumor eradication without toxicity via slow release and local delivery of agonistic CD40 antibody. Clin. Cancer Res. *17*, 2270–2280.

Groom, J.R., and Luster, A.D. (2011). CXCR3 in T cell function. Exp. Cell Res. *317*, 620–631.

Janeway, C.A., Jr. (1992). The T cell receptor as a multicomponent signalling machine: CD4/CD8 coreceptors and CD45 in T cell activation. Annu. Rev. Immunol. *10*, 645–674.

Kaneko, S., Onodera, M., Fujiki, Y., Nagasawa, T., and Nakauchi, H. (2001). Simplified retroviral vector gcsap with murine stem cell virus long terminal repeat allows high and continued expression of enhanced green fluorescent protein by human hematopoietic progenitors engrafted in nonobese diabetic/severe combined immunodeficient mice. Hum. Gene Ther. *12*, 35–44.

Kim, H.J., and Cantor, H. (2014). CD4 T-cell subsets and tumor immunity: the helpful and the not-so-helpful. Cancer Immunol. Res. *2*, 91–98.

Kitayama, S., Zhang, R., Liu, T.Y., Ueda, N., Iriguchi, S., Yasui, Y., Kawai, Y., Tatsumi, M., Hirai, N., Mizoro, Y., et al. (2016). Cellular adjuvant properties, direct cytotoxicity of re-differentiated Valpha24 invariant NKT-like cells from human induced pluripotent stem cells. Stem Cell Rep *6*, 213–227.

Komlosi, Z.I., Kovacs, N., van de Veen, W., Kirsch, A.I., Fahrner, H.B., Wawrzyniak, M., Rebane, A., Stanic, B., Palomares, O., Ruckert, B., et al. (2017). Human CD40 ligand-expressing type 3 innate lymphoid cells induce IL-10-producing immature transitional regulatory B cells. J. Allergy Clin. Immunol. https://doi.org/10.1016/j.jaci.2017.07.046.

Kreiter, S., Vormehr, M., van de Roemer, N., Diken, M., Lower, M., Diekmann, J., Boegel, S., Schrors, B., Vascotto, F., Castle, J.C., et al. (2015). Mutant MHC class II epitopes drive therapeutic immune responses to cancer. Nature *520*, 692–696.

Li, L., Leid, M., and Rothenberg, E.V. (2010). An early T cell lineage commitment checkpoint dependent on the transcription factor Bcl11b. Science *329*, 89–93.

Magri, G., Miyajima, M., Bascones, S., Mortha, A., Puga, I., Cassis, L., Barra, C.M., Comerma, L., Chudnovskiy, A., Gentile, M., et al. (2014). Innate lymphoid cells integrate stromal and immunological signals to enhance antibody production by splenic marginal zone B cells. Nat. Immunol *15*, 354–364.

McKenzie, A.N., Spits, H., and Eberl, G. (2014). Innate lymphoid cells in inflammation and immunity. Immunity *41*, 366–374.

Molldrem, J.J., Lee, P.P., Wang, C., Felio, K., Kantarjian, H.M., Champlin, R.E., and Davis, M.M. (2000). Evidence that specific T lymphocytes may participate in the elimination of chronic myelogenous leukemia. Nat. Med. *6*, 1018–1023.

Naito, T., Tanaka, H., Naoe, Y., and Taniuchi, I. (2011). Transcriptional control of T-cell development. Int. Immunol. *23*, 661–668.

Neofytou, E., O'Brien, C.G., Couture, L.A., and Wu, J.C. (2015). Hurdles to clinical translation of human induced pluripotent stem cells. J. Clin. Invest *125*, 2551–2557.

Nishimura, T., Kaneko, S., Kawana-Tachikawa, A., Tajima, Y., Goto, H., Zhu, D., Nakayama-Hosoya, K., Iriguchi, S., Uemura, Y., Shimizu, T., et al. (2013). Generation of rejuvenated antigen-specific T cells by reprogramming to pluripotency and redifferentiation. Cell Stem Cell *12*, 114–126.

Rezvani, K., Grube, M., Brenchley, J.M., Sconocchia, G., Fujiwara, H., Price, D.A., Gostick, E., Yamada, K., Melenhorst, J., Childs, R., et al. (2003). Functional leukemia-associated antigen-specific memory CD8+ T cells exist in healthy individuals and in patients with chronic myelogenous leukemia before and after stem cell transplantation. Blood *102*, 2892–2900.

Ridge, J.P., Di Rosa, F., and Matzinger, P. (1998). A conditioned dendritic cell can be a temporal bridge between a CD4+ T-helper and a T-killer cell. Nature *393*, 474–478.

Schoenberger, S.P., Toes, R.E., van der Voort, E.I., Offringa, R., and Melief, C.J. (1998). T-cell help for cytotoxic T lymphocytes is mediated by CD40-CD40L interactions. Nature *393*, 480–483.

Sonnenberg, G.F., and Artis, D. (2015). Innate lymphoid cells in the initiation, regulation and resolution of inflammation. Nat. Med. *21*, 698–708.

Spits, H., Artis, D., Colonna, M., Diefenbach, A., Di Santo, J.P., Eberl, G., Koyasu, S., Locksley, R.M., McKenzie, A.N., Mebius, R.E., et al. (2013). Innate lymphoid cells – a proposal for uniform nomenclature. Nat. Rev. Immunol. *13*, 145–149.

Summers deLuca, L., and Gommerman, J.L. (2012). Fine-tuning of dendritic cell biology by the TNF superfamily. Nat. Rev. Immunol. *12*, 339–351.

Tabata, H., Kanai, T., Yoshizumi, H., Nishiyama, S., Fujimoto, S., Matsuda, I., Yasukawa, M., Matsushita, S., and Nishimura, Y. (1998). Characterization of self-glutamic acid decarboxylase 65-reactive CD4+ T-cell clones established from Japanese patients with insulin-dependent diabetes mellitus. Hum. Immunol. *59*, 549–560.

Ueda, N., Zhang, R., Tatsumi, M., Liu, T.Y., Kitayama, S., Yasui, Y., Sugai, S., Iwama, T., Senju, S., Okada, S., et al. (2016). BCR-ABL-specific CD4+ T-helper cells promote the priming of antigen-specific cytotoxic T cells via dendritic cells. Cell. Mol. Immunol *15*, 15–26.

Vizcardo, R., Masuda, K., Yamada, D., Ikawa, T., Shimizu, K., Fujii, S., Koseki, H., and Kawamoto, H. (2013). Regeneration of human tumor antigen-specific T cells from iPSCs derived from mature CD8(+) T cells. Cell Stem Cell *12*, 31–36.

Wakao, H., Yoshikiyo, K., Koshimizu, U., Furukawa, T., Enomoto, K., Matsunaga, T., Tanaka, T., Yasutomi, Y., Yamada, T., Minakami, H., et al. (2013). Expansion of functional human mucosal-associated invariant T cells via reprogramming to pluripotency and redifferentiation. Cell Stem Cell *12*, 546–558.

Wiesel, M., and Oxenius, A. (2012). From crucial to negligible: functional CD8(+) T-cell responses and their dependence on CD4(+) T-cell help. Eur. J. Immunol. *42*, 1080–1088.

Yamada, D., Iyoda, T., Vizcardo, R., Shimizu, K., Sato, Y., Endo, T.A., Kitahara, G., Okoshi, M., Kobayashi, M., Sakurai, M., et al. (2016). Efficient regeneration of human Valpha24+ invariant natural killer T cells and their anti-tumor activity in vivo. Stem Cells *34*, 2852–2860.

Zhang, R., Liu, T., Senju, S., Haruta, M., Hirosawa, N., Suzuki, M., Tatsumi, M., Ueda, N., Maki, H., Nakatsuka, R., et al. (2015). Generation of mouse pluripotent stem cell-derived proliferating myeloid cells as an unlimited source of functional antigen-presenting cells. Cancer Immunol. Res. *3*, 668–677.

Stem Cell Reports, Volume *10*

Supplemental Information

Generation of TCR-Expressing Innate Lymphoid-like Helper Cells that Induce Cytotoxic T Cell-Mediated Anti-leukemic Cell Response

Norihiro Ueda, Yasushi Uemura, Rong Zhang, Shuichi Kitayama, Shoichi Iriguchi, Yohei Kawai, Yutaka Yasui, Minako Tatsumi, Tatsuki Ueda, Tian-Yi Liu, Yasutaka Mizoro, Chihiro Okada, Akira Watanabe, Mahito Nakanishi, Satoru Senju, Yasuharu Nishimura, Kiyotaka Kuzushima, Hitoshi Kiyoi, Tomoki Naoe, and Shin Kaneko

Supplemental Information

Supplemental method

Cells

We isolated peripheral blood mononuclear cells (PBMCs) from healthy donors as described.(Liu et al., 2008) Human monocyte-derived-DCs were induced as described.(Uemura et al., 2009) Human CML cell line K562, human myelogenous leukemia cell line THP-1, and human lung-cancer cell line PC9 were purchased. Mouse L-fibroblasts transfected with HLA class II genes were used as described.(Tabata et al., 1998) For cells isolated from healthy adults, informed consent about their use was obtained from all donors. The entire study was conducted in accordance with the Declaration of Helsinki and with the approval of the appropriate institutional ethics boards.

Transfectants

cDNA encoding *HLA-DR9 (DRB1*09:01)* was previously described.(Ueda et al., 2016) cDNA encoding *BCR-ABL p210* was purchased from Addgene (Cambridge, MA,

USA).(He et al., 2002) cDNA encoding *BCR-ABL p210*, *HLA-A24 (A*24:02)*, *HLA-DRA*, or *HLA-DR9*, or minigene encoding HLA-A24-restricted modified $WT1_{235–243}$ epitope was inserted into lentiviral vector CSII-EF-MCS (RIKEN BioResource Center, Tsukuba, Japan). Lentivirus transduction was performed as described.(Zhang et al., 2015) K562-expressing luciferase gene (K562-Luc) was transduced with lentivirus vectors to express *HLA-A*24:02* and minigene encoding modified $WT1_{235–243}$ epitope (K562-Luc-A24-WT1 minigene). THP-1 was transduced with lentivirus vectors to express *HLA-DRA*01:01* and *HLA-DRB1*09:01* and/or *BCR-ABL p200* (THP-1-DR9, THP1-DR9-BCRABL).

Flow cytometry and antibodies used for functional assays

The monoclonal antibodies (mAbs) used for flow cytometry and functional assays are listed in Table S1. HLA-A*24:02/$WT1_{235-243}$ tetramer was used to detect WT1 peptide-specific CTLs, with HLA-A*24:02/HIV $Env_{584-592}$ tetramer serving as a negative control. The stained cell samples were analyzed using FACSCalibur and FACSAria II flow cytometer (BD Biosciences), and the data were processed using

FlowJo software (Tree Star, Ashland, OR, USA). Relative fluorescence intensity (RFI) was calculated as the ratio of the mean fluorescence intensity (MFI) of specific markers to the MFI of isotype controls.

RNA Sequencing

cDNA was synthesized using a SMARTer Ultra Low Input RNA and sequenced with Illumina Sequencing-HV kit (Clontech, Mountain View, CA, USA), after which the Illumina library was prepared using Low Input Library Prep kit (Clontech). The libraries were sequenced using HiSeq 2500 in 101 cycle Single-Read mode. All sequence reads were extracted in FASTQ format using BCL2FASTQ Conversion Software 1.8.4 in the CASAVA 1.8.2 pipeline. The sequence reads were mapped to hg19 reference genome, downloaded on December 10, 2012, using TopHat v2.0.8b, and quantified using RPKMforGenes. The data have been deposited in NCBI Gene Expression Omnibus (http://www.ncbi.nlm.nih.gov/geo/, accession number GSE94332). Subpopulations from iPS-T cells were obtained on the basis of CD161 and c-Kit expression (Figure S2C), and their gene expression profiles were compared to NK cells,

ILC1s, ILC2s, ILC3s, αβ T cells, and γδ T cells. NK cells, ILC1s, ILC2s, ILC3s, αβ T cells, and γδ T cells were separated from PBMCs of healthy donors (Figure S2D). For pathway analysis, differentially expressed genes were defined by calculating the fold-change of the averaged expression ($|\log2FC| \geq 1$). Hypergeometric tests were conducted using org.Hs.eg.db 3.2.3 of R3.2.2 with GOstats 2.36.0 along with the annotation packages of GO.db 3.2.2 (Gene Ontology analysis) and KEGGprofile 1.12.0 along with the annotation packages of KEGG.db 3.2.2 (KEGG pathway analysis).

Analysis of T cell antigen receptor (TCR) gene rearrangement of T cell clone

The *V*, *D*, and *J* segments of the rearranged TCR-α and TCR-β chains of T cells or iPS-T cells were identified as described.(Uemura et al., 2003) The gene-segment nomenclature used follows the ImMunoGeneTics (IMGT) usage; the *V*, *D*, and *J* segments were identified by comparing the resulting sequences against the IMGT database (http://www.imgt.org/) with an online tool (IMGT/V-QUEST).

Real-time PCR

Total RNA was extracted from iPSCs using an RNeasy Micro kit (Qiagen, Valencia, CA). cDNA was synthesized using High Capacity cDNA Reverse Transcription kits (Applied Biosystems, Foster City, CA, USA) with random 6-mer primers, followed by RT-PCR using ExTaq HS (Takara, Shiga, Japan) and by quantitative-PCR using a TaqMan Array Human Stem Cell Pluripotency Card (Applied Biosystems). Individual PCR reactions were normalized against 18S rRNA.

In vivo bioluminescence imaging

Tumor-bearing mice were injected with 200 μl D-Luciferin (15 mg/ml, VivoGlo Luciferin; Promega, Madison, WI, USA) under 2% inhaled isoflurane anesthesia, and bioluminescent images were obtained using IVIS Lumina II with Living Image Software 3.2 (Xenogen, Alameda, CA, USA).

REFERENCES

He, Y., Wertheim, J.A., Xu, L., Miller, J.P., Karnell, F.G., Choi, J.K., Ren, R., and Pear, W.S. (2002). The coiled-coil domain and Tyr177 of bcr are required

to induce a murine chronic myelogenous leukemia-like disease by bcr/abl. Blood *99*, 2957-2968.

Liu, T.Y., Uemura, Y., Suzuki, M., Narita, Y., Hirata, S., Ohyama, H., Ishihara, O., and Matsushita, S. (2008). Distinct subsets of human invariant NKT cells differentially regulate T helper responses via dendritic cells. European journal of immunology *38*, 1012-1023.

Tabata, H., Kanai, T., Yoshizumi, H., Nishiyama, S., Fujimoto, S., Matsuda, I., Yasukawa, M., Matsushita, S., and Nishimura, Y. (1998). Characterization of self-glutamic acid decarboxylase 65-reactive CD4+ T-cell clones established from Japanese patients with insulin-dependent diabetes mellitus. Human immunology *59*, 549-560.

Ueda, N., Zhang, R., Tatsumi, M., Liu, T.Y., Kitayama, S., Yasui, Y., Sugai, S., Iwama, T., Senju, S., Okada, S.*, et al.* (2016). BCR-ABL-specific CD4+ T-helper cells promote the priming of antigen-specific cytotoxic T cells via dendritic cells. Cell Mol Immunol.

Uemura, Y., Liu, T.Y., Narita, Y., Suzuki, M., Nakatsuka, R., Araki, T., Matsumoto, M., Iwai, L.K., Hirosawa, N., Matsuoka, Y.*, et al.* (2009). Cytokine-dependent modification of IL-12p70 and IL-23 balance in dendritic cells by ligand activation of Valpha24 invariant NKT cells. Journal of immunology *183*, 201-208.

Uemura, Y., Senju, S., Maenaka, K., Iwai, L.K., Fujii, S., Tabata, H., Tsukamoto, H., Hirata, S., Chen, Y.Z., and Nishimura, Y. (2003). Systematic analysis of the combinatorial nature of epitopes recognized by TCR leads to identification of mimicry epitopes for glutamic acid decarboxylase 65-specific TCRs. Journal of immunology *170*, 947-960.

Zhang, R., Liu, T., Senju, S., Haruta, M., Hirosawa, N., Suzuki, M., Tatsumi, M., Ueda, N., Maki, H., Nakatsuka, R.*, et al.* (2015). Generation of mouse pluripotent stem cell-derived proliferating myeloid cells as an unlimited source of functional antigen-presenting cells. Cancer immunology research.

Figure S1

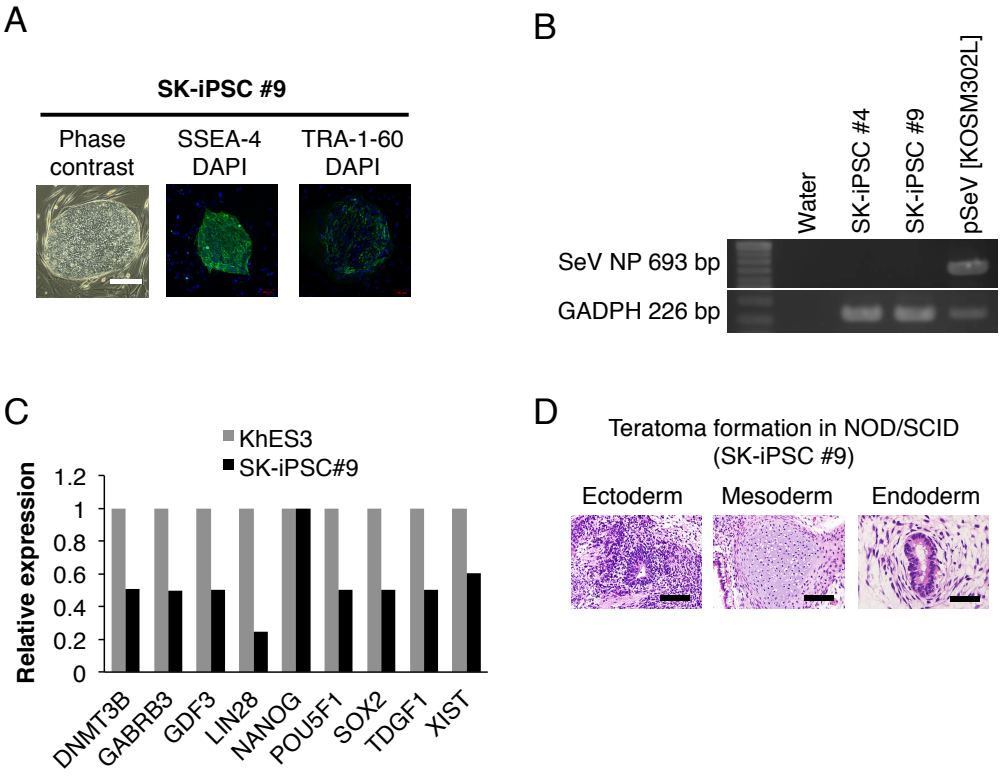

E

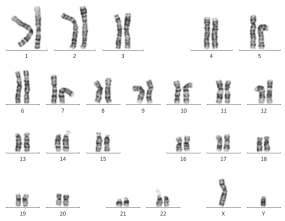

SK-iPSC #9
46XY (20/20)

Figure S2

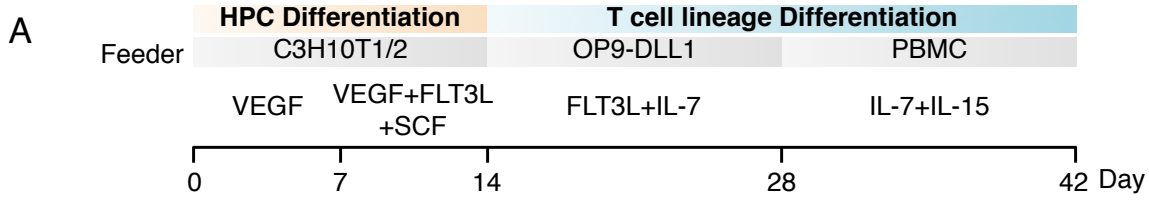

B

SK, Original Th1 Clone

TCRV	FW	CDR3	FW	TCRJ	CDR3 length
*TRAV29/DV5*01*	CAA	SLPQGGSEKL	VFG	*TRAJ57*01*	10
*TRBV2*01*	CAS	SDQGGDNEQ	FFG	*TRBJ2-1*01*	9

iPS-T

TCRV	FW	CDR3	FW	TCRJ	CDR3 length
*TRAV29/DV5*01*	CAA	SLPQGGSEKL	VFG	*TRAJ57*01*	10
*TRBV2*01*	CAS	SDQGGDNEQ	FFG	*TRBJ2-1*01*	9

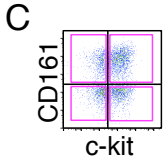

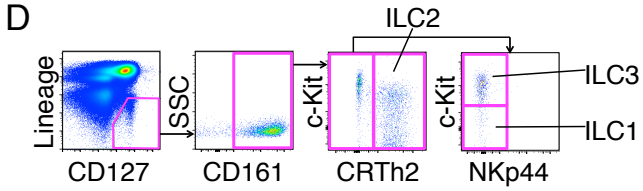

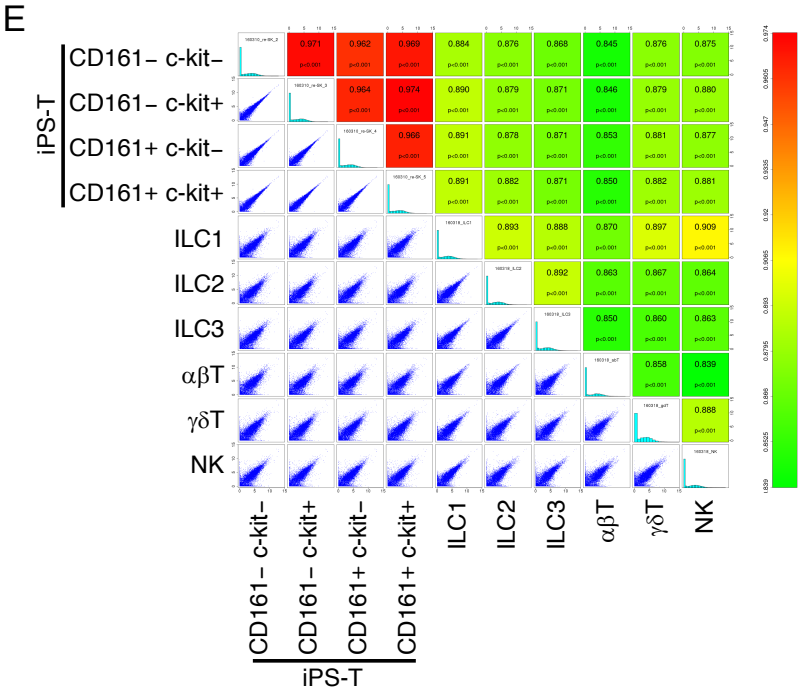

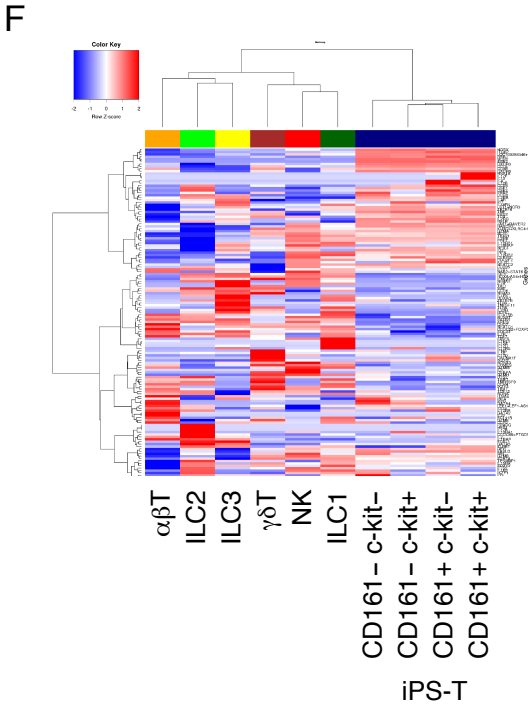

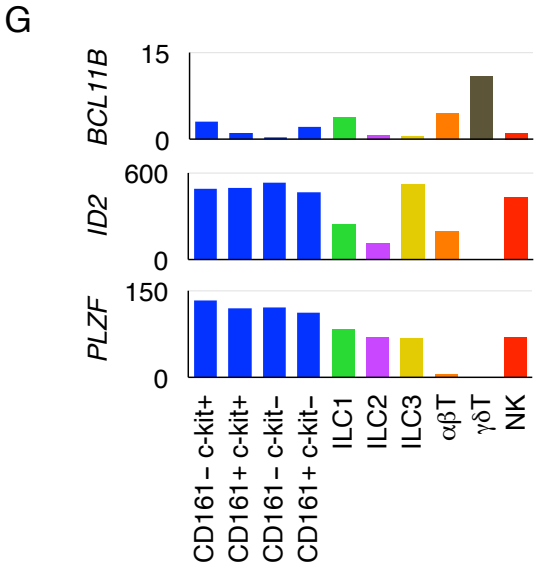

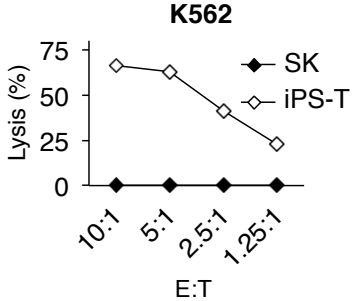

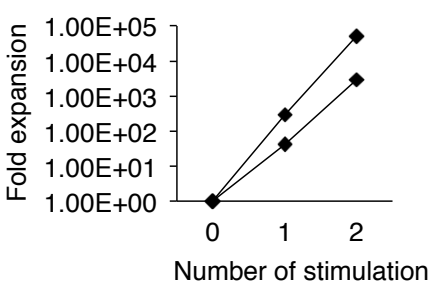

Figure S3

A

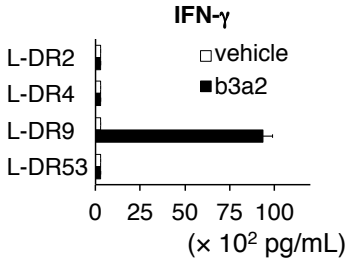

B

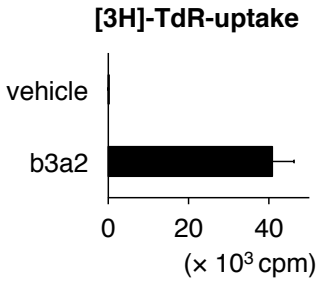

C

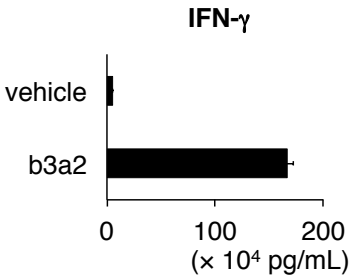

D

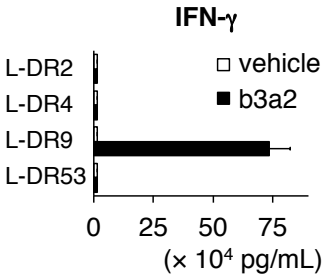

E

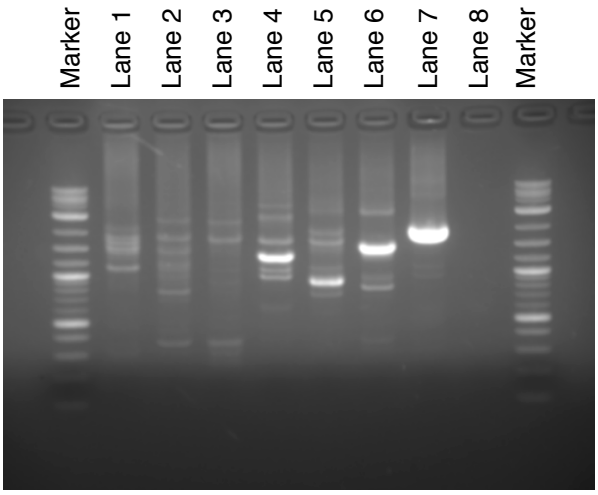

Lane 1: SK CD4+ iPS-T cell Library 1 (DraI digested)
Lane 2: SK CD4+ iPS-T cell Library 2 (SspI digested)
Lane 3: SK CD4+ iPS-T cell Library 3 (HpaI digested)
Lane 4: Retrovirus integrated iPSC clone,TkT3V1-7 Library 1 (DraI digested)
Lane 5: Retrovirus integrated iPSC clone,TkT3V1-7 Library 2 (SspI digested)
Lane 6: Retrovirus integrated iPSC clone,TkT3V1-7 Library 3 (HpaI digested)
Lane 7: Positive control (contained in the kit)
Lane 8: Negative control (H2O)

Figure S4

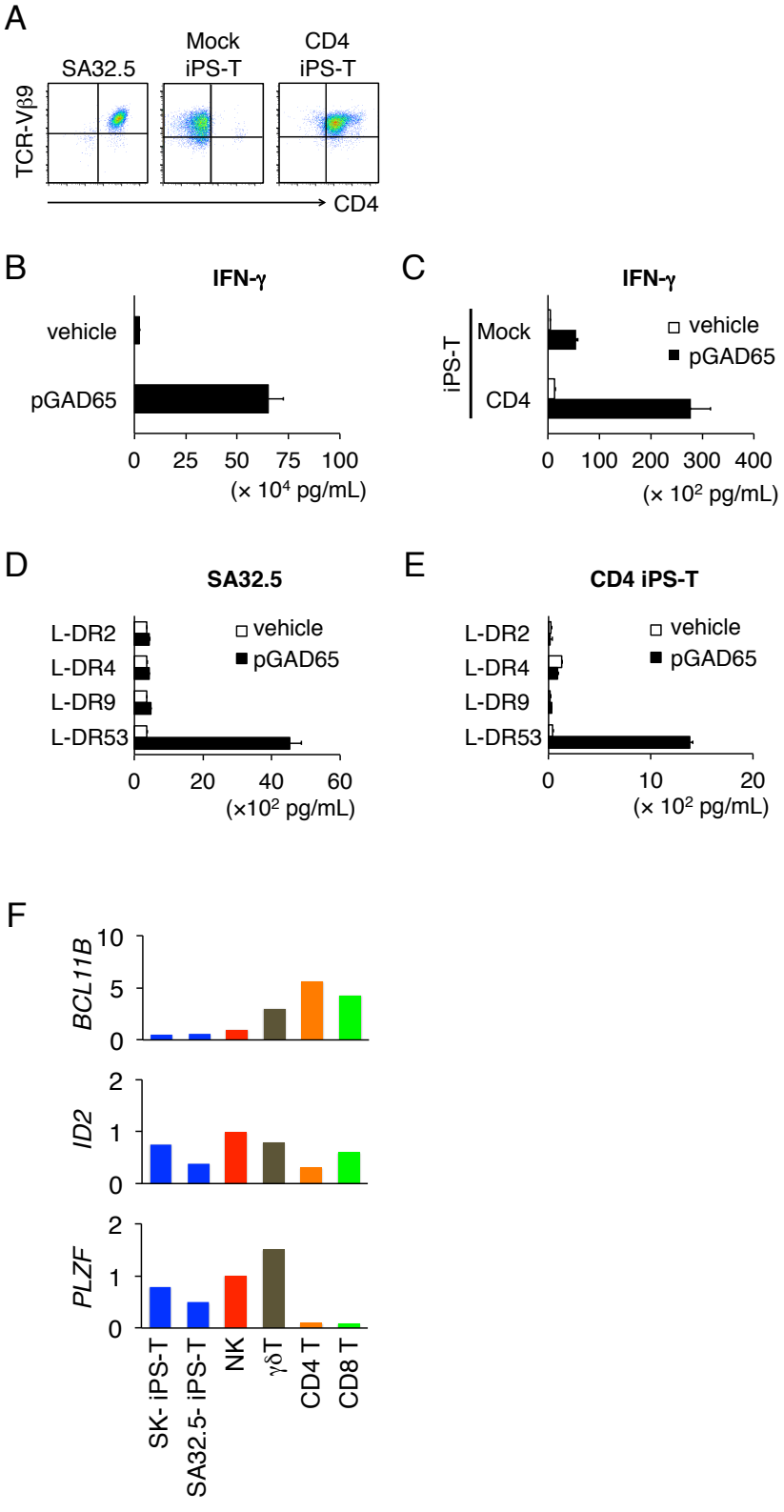
A
SA32.5
Mock iPS-T
CD4 iPS-T
TCR-Vβ9
CD4
B
IFN-γ
vehicle
pGAD65
0 25 50 75 100
(× 10⁴ pg/mL)
C
IFN-γ
iPS-T
Mock
CD4
vehicle
pGAD65
0 100 200 300 400
(× 10² pg/mL)
D
SA32.5
L-DR2
L-DR4
L-DR9
L-DR53
vehicle
pGAD65
0 20 40 60
(×10² pg/mL)
E
CD4 iPS-T
L-DR2
L-DR4
L-DR9
L-DR53
vehicle
pGAD65
0 10 20
(× 10² pg/mL)
F
BCL11B
ID2
PLZF
SK- iPS-T
SA32.5- iPS-T
NK
γδT
CD4 T
CD8 T

Figure S5

A

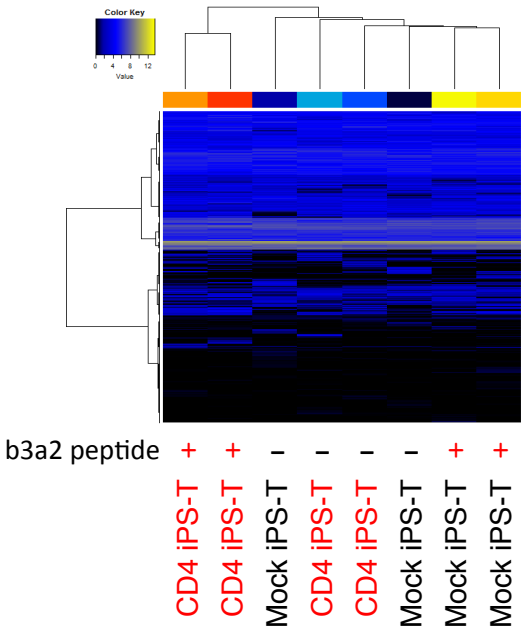

B

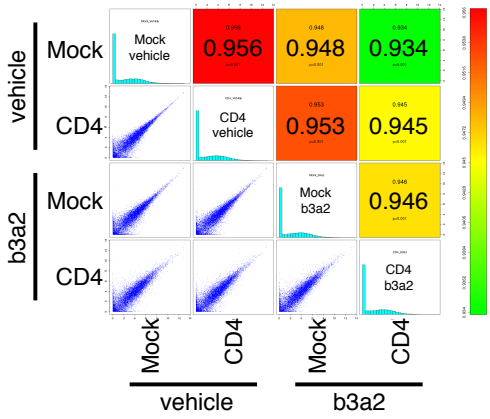

C

GO term	*p* value
Cell proliferation-related gene ontology	
Mitosis	5.47E-14
Nuclear division	5.47E-14
M phase of mitotic cell cycle	8.54E-14
Cell cycle phase	1.4E-13
Organelle fission	1.47E-13
Cell cycle process	2.31E-13
Mitotic cell cycle	7.85E-13

D

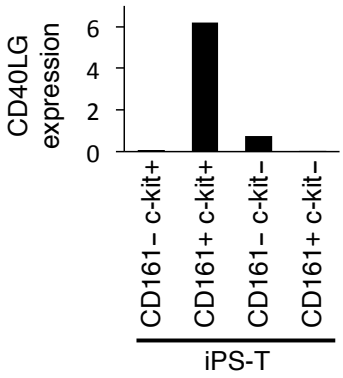

Figure S6

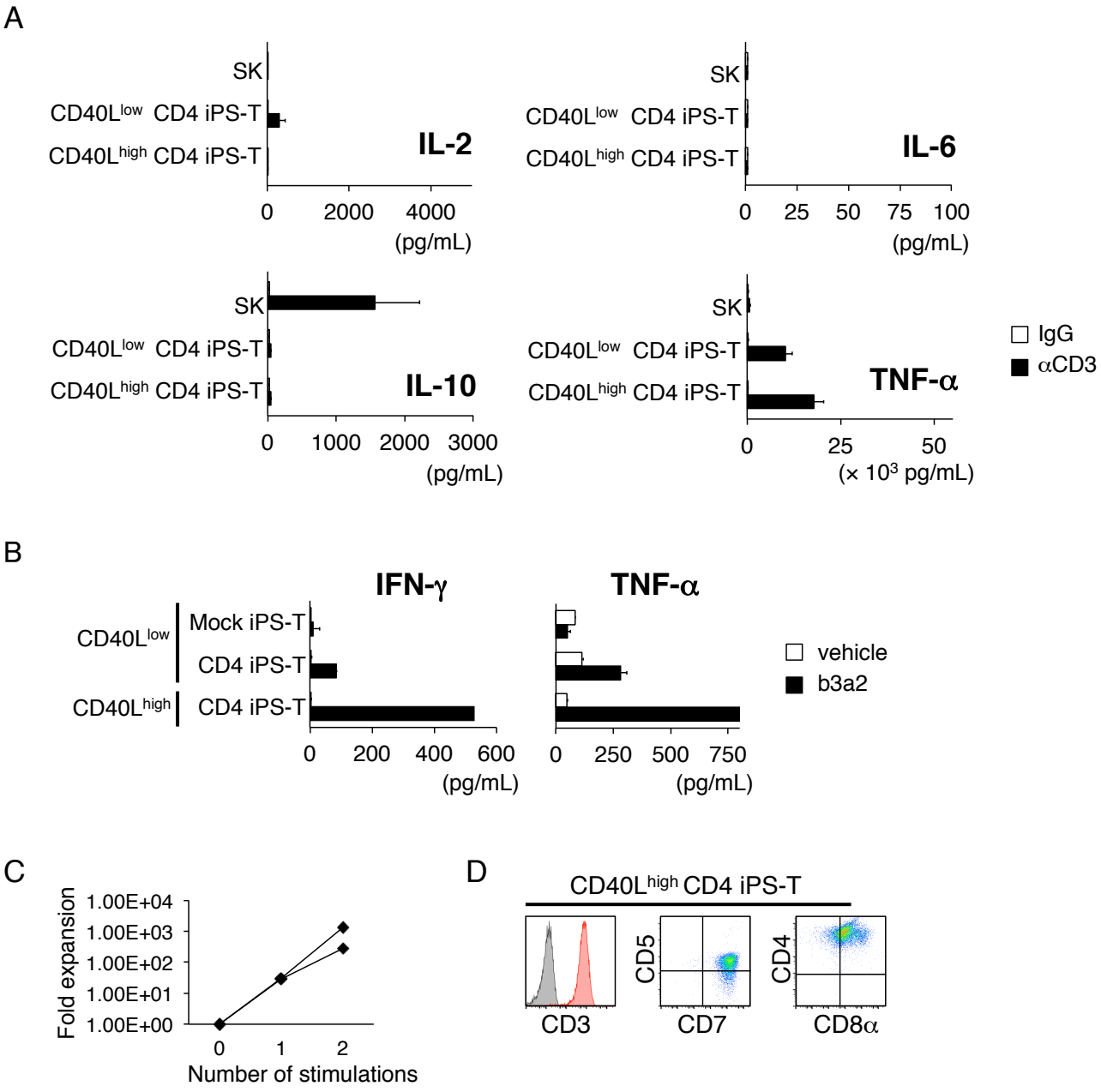
A
SK
CD40L^low CD4 iPS-T
CD40L^high CD4 iPS-T
IL-2
0 2000 4000
(pg/mL)
IL-6
0 25 50 75 100
(pg/mL)
IL-10
0 1000 2000 3000
(pg/mL)
TNF-α
0 25 50
(× 10^3 pg/mL)
IgG
αCD3
B
IFN-γ
TNF-α
CD40L^low
Mock iPS-T
CD4 iPS-T
CD40L^high
CD4 iPS-T
0 200 400 600
(pg/mL)
0 250 500 750
(pg/mL)
vehicle
b3a2
C
Fold expansion
1.00E+04
1.00E+03
1.00E+02
1.00E+01
1.00E+00
0 1 2
Number of stimulations
D
CD40L^high CD4 iPS-T
CD3
CD5
CD7
CD4
CD8α

Figure S7

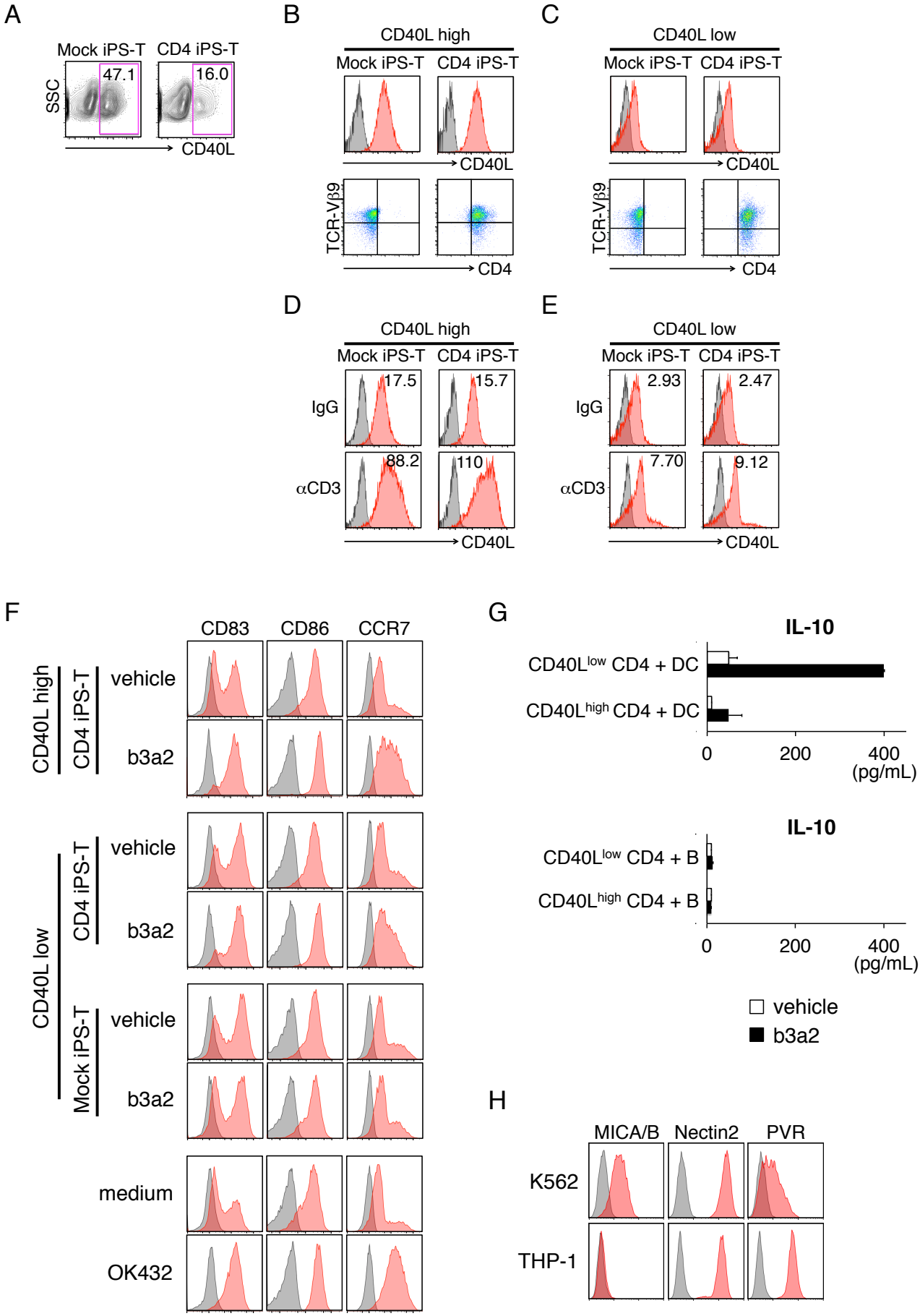
A
Mock iPS-T
CD4 iPS-T
47.1
16.0
SSC
CD40L
B
CD40L high
Mock iPS-T
CD4 iPS-T
CD40L
TCR-Vβ9
CD4
C
CD40L low
Mock iPS-T
CD4 iPS-T
CD40L
TCR-Vβ9
CD4
D
CD40L high
Mock iPS-T
CD4 iPS-T
IgG
17.5
15.7
αCD3
88.2
110
CD40L
E
CD40L low
Mock iPS-T
CD4 iPS-T
IgG
2.93
2.47
αCD3
7.70
9.12
CD40L
F
CD83
CD86
CCR7
CD40L high
CD4 iPS-T
vehicle
b3a2
CD40L low
CD4 iPS-T
vehicle
b3a2
Mock iPS-T
vehicle
b3a2
medium
OK432
G
IL-10
CD40L^low CD4 + DC
CD40L^high CD4 + DC
0
200
400
(pg/mL)
IL-10
CD40L^low CD4 + B
CD40L^high CD4 + B
0
200
400
(pg/mL)
vehicle
b3a2
H
MICA/B
Nectin2
PVR
K562
THP-1

Figure S8

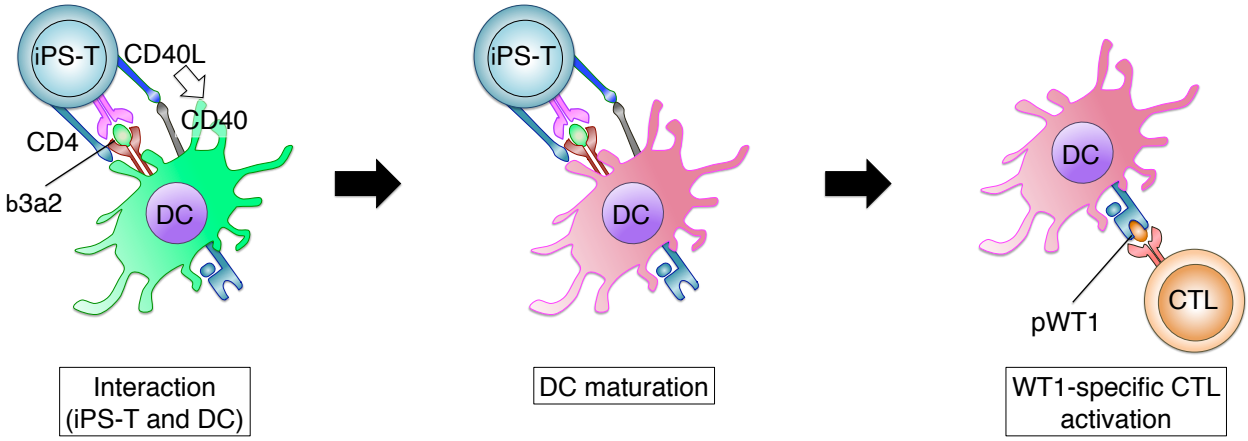
iPS-T
CD40L
CD40
CD4
b3a2
DC
iPS-T
DC
DC
CTL
pWT1
Interaction
(iPS-T and DC)
DC maturation
WT1-specific CTL
activation

Figure S1

Generation of iPSCs from b3a2-specific CD4$^+$ Th1 clone, related to materials and methods

(A) iPSC colonies derived from b3a2-specific CD4$^+$ Th1 clone (SK). Shown are representative phase contrast and immunofluorescent images. Scale bar represents 100 μm. **(B)** PCR-based analysis for detection of SeVdp genomic RNA remnants. Established iPSC colonies from the original CD4$^+$ Th1 clone (SK) (SK-iPSC) did not retain remnant SeVdp (KOSM) 302L vector. **(C)** Quantitative PCR analysis of pluripotency-related genes in SK-iPSCs. Individual PCR results were normalized to 18S ribosomal RNA levels (rRNA). Relative expression values to an embryonic stem cell line (KhES3) are indicated. **(D)** Representative HE-stained sections of a SK-iPSC-derived teratoma from an NOD/ShiJic-scid mouse. iPSCs differentiated into cell lineages derived from endoderm, mesoderm, and ectoderm. Scale bars represent 500 μm. **(E)** Representative karyotype analysis of SK-iPSCs.

Figure S2

Characteristics of T-lineage cells from CD4$^+$ Th1 clone-derived iPSCs, related to Figure 1

(A) Culture protocol for re-differentiation of T-lineage cells from CD4$^+$ Th clone-derived iPSCs. **(B)** TCR gene usage and *V*-(*D*)-*J* junction region sequences of the original CD4$^+$ Th1 clone (SK) and iPS-T cells. **(C)** CD161 and c-Kit expression profiles on iPS-T cells. **(D)** Representative flow cytometry profile of ILC subpopulations from PBMCs of healthy donors. ILC1s, ILC2s, and ILC3s were defined by expression of the indicated molecules. The lineage cocktail contained antibodies for CD1a, CD3, CD11c, CD14, CD19, CD34, CD94, CD123, BDCA2, FcεR1, TCRαβ, and TCRγδ. **(E)** Scatter plots representing the expression of each gene in the indicated pairs of cell types. Numbers in the panels denote pair-wise Pearson's correlation scores. **(F)** Two-way clustering of 146 selected gene expression profiles related to T cell/ILC differentiation and function (Table S3). **(G)** *BCL11B*, *ID2*, and *PLZF* expression in the indicated population. mRNA expression levels were determined by RNA-seq. **(E–G)** Subpopulations from iPS-T cells separated based on CD161 and c-Kit expression shown in (**C**) were compared to NK cells, ILC1s, ILC2s, ILC3s, αβ T cells, and γδ T

cells. **(H)** Cytotoxic activities of original $CD4^+$ Th1 clone (SK) and iPS-T cells to K562 cells. Cytotoxicity was measured by ^{51}Cr-release assay for 4 h at the indicated effector/target (E:T) ratios. Data are representative of two independent triplicate experiments. **(I)** Expansion of iPS-T cells. iPS-T cells were stimulated by PHA-P in the presence of PBMCs at 14-day intervals. Shown are representative results from two independent experiments.

Figure S3

HLA-DR9-restricted, b3a2 peptide-specific response of original $CD4^+$ Th1 clone, related to Figure 1

(A) HLA-DR–restricted IFN-γ production by $CD4^+$ iPS-T cells. $CD4^+$ iPS-T cells (5×10^4) were co-cultured with irradiated L-cell transfectants expressing the indicated HLA-DR (4×10^4) prepulsed with b3a2 peptide (10 μM). **(B)** Proliferative response of the original $CD4^+$ Th1 clone (SK) to antigenic peptide. T cells were co-cultured with autologous PBMCs in the presence of b3a2 peptide (10 μM). Proliferation was determined by the [^{3}H]-thymidine incorporation assay. Data shown are the means ± SD

and are representative of two independent triplicate experiments. **(C)** b3a2 peptide-specific IFN-γ production by the original $CD4^+$ Th1 clone. The original $CD4^+$ Th1 clone (1×10^5) was co-cultured with autologous DCs (5×10^4) that had been prepulsed with the b3a2 peptide (10 μM). **(D)** HLA-DR-restricted IFN-γ production by the original $CD4^+$ Th1 clone. The original $CD4^+$ Th1 clone (5×10^4) was co-cultured with irradiated L-cell transfectants (4×10^4) prepulsed with b3a2 peptide (10 μM). **(A, C, D)** IFN-γ level in the culture supernatant (24 h) was measured by ELISA. Data shown are the means ± SD of triplicate cultures and are representative of two independent experiments. **(E)** Retroviral integration site analysis of $CD4^+$ iPS-T cells by LAM-PCR. Retrovirus-integrated iPSC clone, TkT3V1-7, served as a positive control.

Figure S4

CD4 modification induces HLA class II-restricted responses in iPS-T cells derived from GAD65 peptide-specific $CD4^+$ Th clone, related to Figure 1

(A) Representative flow cytometry profiles of the indicated molecules on GAD65 peptide-specific $CD4^+$ Th clone (SA32.5) and iPS-T cells from SA32.5-derived iPSCs

transduced with Mock or CD4 gene. **(B)** GAD65 peptide-specific IFN-γ production by SA32.5. **(C)** GAD65 peptide-specific IFN-γ production by mock iPS-T cells and $CD4^+$ iPS-T cells, both from SA32.5-derived iPSCs. **(B, C)** IFN-γ level in the culture supernatant was measured by ELISA. SA32.5, mock iPS-T cells, or $CD4^+$ iPS-T cells (1×10^5) were co-cultured for 24 h with HLA-DR53 positive DCs (5×10^4) that had been prepulsed with GAD65 peptide (10 μM). Data shown are the means ± SD and are representative of two independent triplicate experiments. **(D)** HLA-DR-restricted IFN-γ production by SA32.5. **(E)** HLA-DR-restricted IFN-γ production by $CD4^+$ iPS-T cells from SA32.5-derived iPSCs. **(D, E)** IFN-γ level in the culture supernatant (24 h) was measured by ELISA. SA32.5 or $CD4^+$ iPS-T cells (5×10^4) were co-cultured with irradiated L-cell transfectants (4×10^4) that had been prepulsed with GAD65 peptide (10 μM). Data shown are the means ± SD of triplicate cultures and are representative of two independent experiments. **(F)** Measurement of *BCL11B*, *ID2*, and *PLZF* mRNA expression by real-time RT-PCR in the indicated population. Expression of each mRNA was normalized to that of *ACTB* mRNA (SK-iPS-T: iPS-T cells derived from b3a2-specific $CD4^+$ Th1 clone (SK), SA32.5-iPS-T: iPS-T cells derived from GAD65

peptide-specific $CD4^+$ Th clone (SA32.5)).

Figure S5

Gene expression of CD4 modified iPS-T cells, related to Figure 1

(A) Two-way clustering showing global gene expression profiles. Mock iPS-T cells and $CD4^+$ iPS-T cells were stimulated with vehicle or b3a2 peptide. THP-1-expressing HLA-DR9 was used as APCs. **(B)** Scatter plots representing the expression of each gene in the indicated pairs of cell types. Numbers in the panels denote pair-wise Pearson's correlation scores. **(C)** Gene ontology (GO) term enriched in genes significantly up-regulated in b3a2-stimulated $CD4^+$ iPS-T cells compared to in b3a2-stimulated Mock iPS-T cells. **(A–C)** Mock iPS-T cells and $CD4^+$ iPS-T cells were stimulated with vehicle or b3a2 peptide. THP-1-expressing HLA-DR9 were used as APCs. **(D)** CD40L gene expression of subpopulations from iPS-T cells. mRNA expression levels were determined by RNA-seq.

Figure S6

Function and surface phenotype of CD40L^{high} population from CD4^{+} iPS-T cells, related to Figure 2

(A) Cytokine production by the indicated populations. Each population was stimulated with plate-bound control IgG or anti-CD3 mAb (10 μg/mL). The original CD4^{+} Th1 clone (SK) served as a control. **(B)** Cytokine production by the indicated populations. Each population (1×10^4) was co-cultured with autologous DCs (2.5×10^4) that had been prepulsed with b3a2 peptide (10 μM). **(A–B)** Cytokine levels in the culture supernatant (24 h) were measured in a bead-based multiplex immunoassay. Data shown are the means ± SD of triplicate cultures and are representative of two independent experiments. **(C)** Expansion of CD40L^{high} CD4^{+} iPS-T cells. CD40L^{high} CD4^{+} iPS-T cells were stimulated with PHA-P in the presence of PBMCs at 14-day intervals. Shown are representative results of two independent experiments. **(D)** Representative flow cytometry profiles of the indicated molecules on CD40L^{high} and CD40L^{low} CD4^{+} iPS-T cells. Indicated surface molecules (red) and isotype-matched controls (gray) are shown.

Figure S7

CD40L^{high} CD4^{+} iPS-T cells derived from SA32.5-iPSCs, related to Figure 2-4

(A) Representative flow cytometry profiles of the indicated molecules on the indicated iPS-T cells from SA32.5-iPSCs on day 13 after PHA-P stimulation. The number of CD40L-positive cells is shown in the upper right corner of each panel. Mock iPS-T cells or CD4^{+} iPS-T cells were stimulated with PHA-P, cultured for 12 days in the presence of IL-7 and IL-15, and then cultured for 24 h in the presence of IL-2 and IL-15. **(B, C)** Expressions of CD40L, CD4, and TCR-Vβ9 on each subpopulation are shown. CD40L high and low populations were separated from Mock iPS-T cells or CD4^{+} iPS-T cells by flow cytometry sorting and expanded by PHA-P stimulation. **(D, E)** Surface CD40L expression on different subpopulations stimulated with plate-bound control IgG or anti-CD3 mAb (10 μg/mL). The original CD4^{+} Th clone (SA32.5) served as a control. Relative fluorescence intensity (RFI) is shown in the upper right corner of each panel. **(B–E)** CD40L (red) and isotype-matched controls (gray) are shown. **(F)** Representative flow cytometry profiles of the indicated molecules on DCs. Vehicle- or b3a2-peptide-pulsed DCs were cultured for 24 h with the indicated population at a DC/CD4^{+} iPS-T cell ratio of 5:1. OK432 (10 μg/mL)-matured DCs and medium-control

DCs served as controls. The indicated surface molecules (red) and isotype-matched controls (gray) are shown. **(G)** IL-10 production by DCs or B cells co-cultured with the indicated population. IL-10 in the culture supernatant was measured by ELISA. The indicated population (2×10^4) was co-cultured for 24 h with autologous DCs or B cells (5×10^4) that had been prepulsed with b3a2 peptide (10 μM). Data shown are the means ± SD of triplicate cultures and are representative of two independent experiments. **(H)** Representative flow cytometry profiles of the indicated molecules on K562 and THP-1.

Figure S8

Mechanism of the WT1-specific CTL priming via DC maturation by iPS-T cells, related to Figure 5

Mechanism of the WT1-specific CTL priming. b3a2, b3a2 peptide; pWT1, WT1 peptide. **(left panel)** When iPS-T cells recognize b3a2 peptide presented by DCs, the activated iPS-T cells up-regulate CD40L. **(center panel)** CD40 ligation by CD40L induces DC maturation. **(right panel)** Up-regulation of costimulatory molecules and enhanced cytokine production by DCs promote activation of WT1 peptide-specific CTLs.

Table S1

Antigen	Clone	Isotype
CD1a	HI149	mouse IgG1
CD3	OKT3	mouse IgG2a
CD3	UCHT1	mouse IgG1
CD4	OKT-4	mouse IgG2b
CD4	RPA-T4	mouse IgG1
CD5	UCHT2	mouse IgG1
CD7	CD7-6B7	mouse IgG2a
CD8 α	SK1	mouse IgG1
CD8 β	2ST8.5H7	mouse IgG2a
CD11c	MJ4-27G12	mouse IgG2b
CD14	M5E2	mouse IgG2a
CD19	HIB19	mouse IgG1
CD34	581	mouse IgG1
CD40	HB14	mouse IgG1
CD45	HI30	mouse IgG1
CD56	HCD56	mouse IgG1
CD80	2D10	mouse IgG1
CD83	HB15a	mouse IgG2b
CD86	IT2.2	mouse IgG2b
CD94	REA113	recombinant human IgG1
CD117 (c-Kit)	104D2D1	mouse IgG1
CD123	6H6	mouse IgG1
CD127	HIL-7R-M21	mouse IgG1
CD154 (CD40L)	24-31	mouse IgG1
CD161	HP-3G10	mouse IgG1
CD197 (CCR7)	G043H7	mouse IgG2a
CD226 (DNAM-1)	11A8	mouse IgG1
CD279 (PD-1)	EH12.2H7	mouse IgG1
CD294 (CRTh2)	BM16	rat IgG2a
CD303 (BDCA2)	AC144	mouse IgG1
CD314 (NKG2D)	1D11	mouse IgG1
CD335 (NKp46)	9E2	mouse IgG1
CD336 (NKp44)	P44-8	mouse IgG1
CD337 (NKp44)	P30-15	mouse IgG1
Fc ε R1	AER-37	mouse IgG2b
HLA-DR	L243	mouse IgG2a
TCR- α β	IP26	mouse IgG1
TCR- γ δ	B1.1	mouse IgG1
TCRBV9S1	FIN9	mouse IgG2a
TRBV22S1	IMMU546	mouse IgG1

Isotype control	Clone
mouse IgG1	MOPC-21
mouse IgG1	P3.6.2.8.1
mouse IgG2a	G155-178
mouse IgG2b	eBMG2b

Table S2

Pearson's correlation of gene expression between iPS-T cell samples and other cell types

Sample	Pearson correlation
iPS-Ts	0.962-0.974
NK	0.875-0.881
ILC1	0.884-0.891
ILC2	0.876-0.882
ILC3	0.868-0.871
α/β-T	0.845-0.853
γ/δ-T	0.876-0.882

Table S3

AHR	AREG	ASB2	BCL11B	CACNA1F	CCL5	CCL7	CCR3	CCR4	CCR5
CCR6	CCR7	CD226	CD3E	CEBPA	CEBPB	CHD7	CSF1	CSF2	CXCR3
CXCR6	EOMES	ETS1	ETS2	FASLG	FOSL1	FOXP3	GATA2	GATA3	GATA4
GFI1	GZMA	GZMB	GZMH	GZMK	GZMM	HAVCR2	HES1	HNF1A	HOPX
HOXA10	HOXA3	ICOS	ID2	ID3	IFNG	IFNGR1	IGSF6	IKZF1	IKZF2
IKZF3	IL10	IL12A	IL12B	IL12RB1	IL12RB2	IL13	IL13RA1	IL15RA	IL17A
IL17B	IL17C	IL17D	IL17F	IL17RB	IL17RE	IL18	IL18R1	IL18RAP	IL1R1
IL1R2	IL1RAP	IL1RL1	IL2	IL21	IL22	IL23R	IL2RA	IL2RB	IL2RG
IL4	IL4R	IL5	IL7R	IL9	IRF1	IRF4	IRF8	ITGAE	ITGB7
JAK1	KIF2C	KIT	KLRB1	KLRK1	LEF1	LRRC32	MAF	MYB	NCAM1
NCR1	NCR2	NCR3	NFATC1	NFATC2	NFIL3	NR4A1	NR4A3	PERP	PKD2
POU2F2	PPARG	PRF1	PTGDR2	RBPJ	REL	RELB	RORA	RORC	RUNX1
RUNX3	SATB1	SOCS1	SOCS5	SOX13	STAT1	STAT4	STAT5B	STAT6	TAL1
TBX21	TCF12	TCF7	TGIF1	THY1	TIGIT	TLR4	TLR6	TNF	TNFRSF9
TNFSF11	TOX	TP53INP1	UTS2	ZBTB16	ZBTB7B				

Table S4

Category	Term	Count	%	P-Value	Genes	List Total	Pop Hits	Pop Total	Fold Enrichment	Bonferroni
KEGG_PATHWAY	hsa04650:Natural killer cell mediated cytotoxicity	6	2.205882353	1.23E-05	PRF1, KLRK1, FASLG, GZMB, NFATC2, NCR1	14	133	5085	16.38560687	2.72E-04
KEGG_PATHWAY	hsa04630:Jak-STAT signaling pathway	5	1.838235294	4.79E-04	IL12RB2, IL2RB, STAT4, IL12RB1, JAK1	14	155	5085	11.71658986	0.01048484
KEGG_PATHWAY	hsa05330:Allograft rejection	3	1.102941176	0.003619614	PRF1, FASLG, GZMB	14	36	5085	30.26785714	0.076676827
KEGG_PATHWAY	hsa05332:Graft-versus-host disease	3	1.102941176	0.004238978	PRF1, FASLG, GZMB	14	39	5085	27.93956044	0.089221673
KEGG_PATHWAY	hsa04940:Type I diabetes mellitus	3	1.102941176	0.004904194	PRF1, FASLG, GZMB	14	42	5085	25.94387755	0.102513944
KEGG_PATHWAY	hsa05320:Autoimmune thyroid disease	3	1.102941176	0.007168701	PRF1, FASLG, GZMB	14	51	5085	21.36554622	0.146388778
KEGG_PATHWAY	hsa04060:Cytokine-cytokine receptor interaction	4	1.470588235	0.026326675	IL12RB2, IL2RB, IL12RB1, FASLG	14	262	5085	5.54525627	0.443977985

Table S5

Pearson correlation of gene expressions.

Cell samples		Pearson correlation
CD4 b3a2	Mock vehicle	0.934
	CD4 vehicle	0.945
	Mock b3a2	0.946
Mock vehicle	CD4 vehicle	0.956
	Mock b3a2	0.953
CD4 vehicle	Mock b3a2	0.948